



Photon: Federated LLM Pre-Training

Lorenzo Sani^{1,2,†} Alex Iacob^{1,2} Zeyu Cao¹ Royson Lee¹ Bill Marino¹

Yan Gao^{1,2} Dongqi Cai^{1,3} Zexi Li^{1,4} Wanru Zhao¹ Xinchu Qiu¹

Nicholas D. Lane^{1,2}

Abstract

Scaling large language models (LLMs) demands extensive data and computing resources, which are traditionally constrained to data centers by the high-bandwidth requirements of distributed training. Low-bandwidth methods like federated learning (FL) could enable collaborative training of larger models across weakly-connected GPUs if they can effectively be used for pre-training. To achieve this, we introduce *Photon*, the first complete system for federated end-to-end LLM training, leveraging cross-silo FL for global-scale training with minimal communication overheads. Using *Photon*, we train the first federated family of decoder-only LLMs from scratch. We show that: (1) *Photon* can train model sizes up to 7B in a federated fashion while reaching an even better perplexity than centralized pre-training; (2) *Photon* model training time decreases with available compute, achieving a similar compute-time trade-off to centralized; and (3) *Photon* outperforms the wall-time of baseline distributed training methods by 35% via communicating $64\times$ – $512\times$ less. Our proposal is robust to data heterogeneity and converges twice as fast as previous methods like DiLoCo. This surprising data efficiency stems from a unique approach combining small client batch sizes with extremely high learning rates, enabled by federated averaging’s robustness to hyperparameters. *Photon* thus represents the first economical system for global internet-wide LLM pre-training.

1 Introduction

Trends in developing state-of-the-art large language models (LLMs) suggest training ever-larger models on expanding datasets with growing compute resources [1, 2]. The standard approach involves using a mix of distributed learning algorithms with high-bandwidth communication requirements deployed in single data center, e.g., distributed data parallelism across racks, pipeline parallelism across servers in a rack, and tensor parallelism across GPUs in a server [3–6]. Thus, increasing model

¹Department of Computer Science and Technology, University of Cambridge

²Flower Labs

³Beijing University of Posts and Telecommunications

⁴Zhejiang University

[†]Corresponding author: ls985@cam.ac.uk

size requires extending computing facilities to exploit high-bandwidth distributed training algorithms [7, 8].

Recently, a small but growing interest in low-bandwidth distributed training algorithms has developed to exploit the worldwide distribution of computing facilities connected through the Internet [9–14]. If successful, low-bandwidth distributed training could overcome the need to build more extensive data centers. The federated learning (FL) approach [15] is appealing as an additional layer of parallelism across poorly connected nodes, such as data centers distributed in different regions [9, 16–18] or internet-wide collaborative training. The reasons for its appeal are three-fold: (1) FL optimizers derive from LocalSGD [19], which allows more infrequent synchronization compared to distributed data parallelism; (2) the size of text datasets makes it challenging to replicate across data centers [3]; and (3) federations scale seamlessly as participants join [20].

In this work, we present *Photon*, the first open-source FL system for executing pre-training of LLMs across a distributed setting - composed of individuals privately owning a handful of hardware accelerators - communicating through the Internet. We show that SystemX effectively navigates the trade-off between performance and efficiency and fills the gap for researchers and practitioners to federatedly pre-train high-performance LLMs off the shelf. Notably, *Photon* has been used for pre-training the *first* family of federated decoder-only large language models *from scratch*, scaling model size up to 7B. Moreover, academic and industry researchers have used *Photon* to execute 1811 experiments and submit six papers to international machine-learning venues. We built *Photon* on the `FLower` framework and published its complete implementation at this repository.

The contributions of this work are the following:

1. We introduce *Photon*, the first open-source system for federated LLM pre-training over the Internet, enabling collaboration across private GPUs or distributed subsets of data centers worldwide. *Photon* has successfully trained the first federated family of decoder-only LLMs from scratch, reaching lower perplexities than centralized training for models up to 7B parameters.
2. We show that *Photon* achieves up to 20% higher throughput (samples/sec) than centralized distributed training, requiring $64 \times -512 \times$ less communication.
3. We propose a novel federated pre-training approach exploiting the robustness to hyperparameters of federated averaging in order to combine small device batch sizes with high learning rates. This allows models trained with *Photon* to converge twice as fast as previous methods, such as DiLoCo [9].
4. By combining high throughput with our optimization method, we demonstrate that training time with *Photon* reduces as more compute resources are added up to a certain batch size limit. This achieves a compute-time trade-off similar to centralized pre-training.

2 LLM pre-training under Decentralized System Conditions

We focus on low-bandwidth distributed settings for training LLM. In such scenarios, the standard distributed training method of synchronizing gradients at every batch step would incur very high overheads. For example, the inter-worker communication costs of using distributed data parallelism (DDP) with *Ring-AllReduce* [21] would be $\mathcal{O}(|\theta| \times T)$ where $|\theta|$ is the model size and T is the number of training steps. Moving to federated training allows us to reduce the communications costs [19, 22] to $\mathcal{O}(|\theta| \times \frac{T}{T_{\text{local}}})$ by performing T_{local} steps on a “worker” prior to synchronization.

While highly beneficial from a communication perspective, infrequent synchronization significantly alters the optimization procedure [19, 23, 24]. Every gradient descent step in standard distributed training is executed on a fully up-to-date model. At the same time, in federated learning, participants operate with stale parameters for T_{local} steps. This poses challenges to reaching a similar level of data efficiency as standard distributed training [25]. In addition to this fundamental challenge, various FL settings can pose additional difficulties, such as hardware and data heterogeneity [22].

2.1 Emerging Decentralized Scenarios

Our design space has three particular settings for which low-bandwidth training methods are likely beneficial.

Cross Data-center: This scenario resembles standard distributed training, where multiple data centers collaborate to train models even larger than the current SOTA. Typically, distributed training approaches cannot operate over the low-bandwidth connection across data centers, forcing corporations to build ever-larger facilities.

Cross-silo: Here, we assume collaboration among several small organizations, each equipped with one to eight high-performance accelerators. In such cases, not only is the bandwidth across silos low, but silos may have an insufficient number of GPUs to saturate the batch-size requirements of even modest-sized models.

Collaboration via Commodity Hardware: In this setup, individuals with a small number of consumer-grade GPUs collaborate in model training. This setting presents the above challenges in a harsher form due to strong VRAM constraints on commodity GPUs, making it difficult even to train a model without extreme CPU offloading.

Collaborating in such federated scenarios aims to benefit from *more computing power and data sources* by *achieving the machine learning (ML) optimization objective* quicker than what standard training can do in a single location. Given our available resources, we focus on the standard cross-silo setting. Thus, we *assume* that every participant possesses the following minimal requirements: (a) one or many well-connected hardware accelerators, which can be sporadically available throughout a full training cycle; (b) sufficient memory to train the full model with a pre-defined small (local) batch size; (c) access to a pre-tokenized text corpus, either stored in the same facility or streamed through the Internet from a private data silo; and (d) a stable connection to the Internet with an average bandwidth of 2.5Gbps.

2.2 Computation Efficiency

LLM pre-training has presented many challenges to systems and architecture designers, as it has unprecedented memory footprints (VRAM) and requires extensive computing capabilities (FLOP-s/s) [26]. Most of these are mitigated by pooling extensive hardware accelerators and adopting distributed training algorithms. Standard distributed training algorithms are based on 3D parallelism, which applies data parallelism (DP) across racks in a data center [27], pipeline parallelism (PP) across servers in a rack [28], and tensor parallelism (TP) across GPUs in a server [29]. The common practice is designing computing facilities to fully exploit 3D parallelism for optimal resource utilization.

Achieving optimal resource utilization requires thoughtful configuration of the hyperparameters and the mixture of distributed algorithms, which becomes more challenging as the scale increases. This tuning involves choosing the most appropriate batch size that will result in the least expensive gradient accumulation (ideally, none). We assume the participants in the distributed settings discussed here thoroughly understand their available hardware and their interplay with the 3D parallelism of the target model size. We construct our evaluation on settings running full batch steps matching their resources without any gradient accumulation.

2.3 Sourcing and Moving Data

ML workloads, such as LLM pre-training, require massive training data and computational resources, naturally distributed across several regions. To achieve reasonable efficiency, ML infrastructures are designed to follow the *data-GPU collocation* principle, i.e., data warehouses are colocated in the same region with GPU clusters to avoid relying on the cross-region network bandwidth (usually 10 times lower than intra-region network bandwidth). Large-scale infrastructures face the challenge of satisfying *data-GPU collocation* for *exabytes* of data, tens of regions with thousands of GPUs. Data is also continuously produced and removed, making the collocation task even more challenging. A worldwide scheduler, such as MAST [3], optimizes the cross-regional data placement daily, leveraging algorithms that can take up to 5 hours to complete their task. In this context, our work tackles a setting, usually referred to as *training-at-home*. Our *Photon* takes advantage of the available computing power at clients, where data is stored, resulting in the following benefits: (a) it doesn't require particular data placement optimization; (b) it can leverage low-hanging fruit local storage optimizations, such as data pre-tokenization, (c) it is compliant with privacy constraints as it doesn't move data.

2.4 Cross-silo Communication

Training procedures based on 3D parallelism leverage high-bandwidth networks supported by *intra-datacenter* networking solutions such as RoCE and InfiniBand with the typical link speed from 100Gbps up to 400Gbps per link. [30–32]. Their communication efficiency of the standard distributed training approach is heavily impacted by slow network links, which makes them unsuitable for *cross-region* applications we are interested in as their network bandwidth ranges from 0.8Gbps to 40Gbps. In this work, we use distributed training algorithms based on LocalSGD, which requires less frequent communication across workers [33] and strongly reduces the overheads of possessing slower links across workers.

3 Architecture and Design of *Photon*

To enable collaborative and effective cross-silo FL pre-training of LLMs with limited inter-data center communication, *Photon* follows three core principles: *broad inclusivity of data and compute sources*, *minimal compute requirements*, and *scalable local training pipelines*. These principles maximize client resource utilization and ensure a robust design. We now present *Photon*’s architecture, beginning with a brief overview of its core innovations. The main components are summarized in Figure 1(a).

Adaptive Local Parallelism: *Photon* integrates standard distributed training techniques with federated learning, optimizing training data storage, transfer, parameter communication, and aggregation. It adapts to each client’s connectivity and topology, allowing automatic selection between standard distributed training and low-bandwidth LocalSGD.

Improved Model Generalization: The federated optimization we adopt produces robust model minima and is resilient to hyperparameter variations due to noise injection [24] and meta-learning effects [34], ensuring convergence across varied client participation levels, data heterogeneity, and local training hyperparameters. Since robust model minima, defined as model parameters whose loss does not significantly change upon perturbation, are known to generalize better and produce lower validation loss [35, 24], this partially explains the outperformance that models trained with *Photon* show over centralized pre-training.

Exploiting Small Batches and High Learning Rates: *Photon*’s robustness to hyperparameter choices enables the use of **small** (hardware-determined) local batch sizes, which promote flat minimizers of the loss that generalize better [35], along with **high learning rates** decayed over an extended period—typically unstable with small batches—allowing us to maintain data efficiency. For example, if centralized training uses a decay period T with batch size \mathcal{B} , federated learning enables us to extend it to $T \times \frac{\mathcal{B}}{\mathcal{B}_{\text{small}}}$. In our experiments, using small batch sizes $\mathcal{B}_{\text{small}}$ in centralized training always resulted in model divergence unless the maximal learning rate was reduced linearly w.r.t the batch size. Full details are in Appendix C.1.

3.1 Architecture

Photon consists of the following core components.

Aggregator (Agg): Agg serves as the central server orchestrating the federated training process. At the start of each round, it activates the *Client Sampler* to access and select LLM-C instances according to the optimization algorithm’s requirements. Agg then uses Link to relay messages between LLM-C clients. Once results are received from LLM-C, `OuterOpt` aggregates updates and applies the optimization to the global model, followed by checkpointing.

LLM Client (LLM-C): LLM-C is the distributed client in *Photon* responsible for the local training pipeline within the federated optimization process. Each LLM-C can connect to Agg at any point during training. The `ClientOpt` trains the model received from Agg on local data, utilizing various distributed algorithms suited to each LLM-C’s hardware capabilities. Model updates and training metadata are then exchanged with Agg through Link. The training state is regularly checkpointed for fast recovery in case of failure.

Data Sources (DS): Data Sources serve as the data storage for *Photon*, meeting the federated learning requirements regarding data location and exchange protocols. Each private DS is linked to

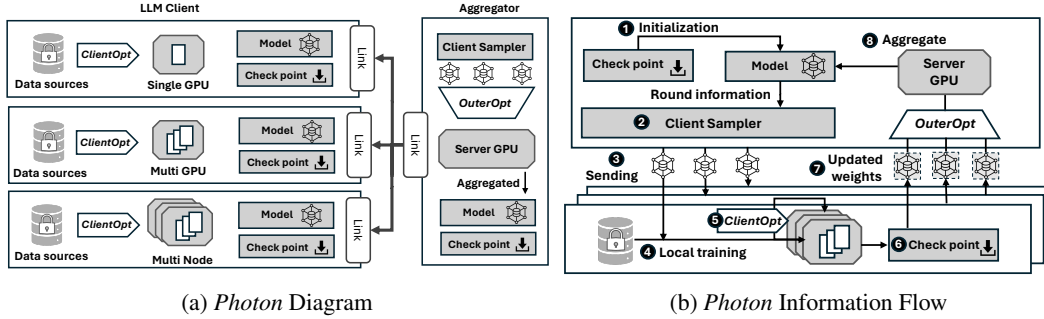


Figure 1: **(a) Systematic diagram of *Photon*'s three principal components - *Photon* aggregator, *Photon* LLM clients, and *Photon* data sources.** Arrows describe interactions and message exchanges. The *Photon* aggregator can only communicate with the *Photon* LLM nodes through the *Photon* link. The instances responsible for storing the data samples, the *Photon* data sources, can uniquely stream to the *Photon* client bound to them. **(b) Information flows between LLM clients, the aggregator, and data sources.** Following initialization (1), An LLM client selected by the client sampler (2) receives model parameters from the server (3), trains on data from a data source (4,5), checkpoints (6), and then returns the updated parameters (7) to the aggregator for federated optimization (8).

an individual LLM-C within the same client's data domain, generating a continuous data stream that matches `ClientOpt`'s training throughput. This decoupled structure allows institutions with large data silos to obtain paired computation through LLM-C without sharing data globally. Additionally, public DS can be configured for data sharing among LLM-C clients to support collaboration or data-sharing agreements between participants.

3.2 Operation

We detail *Photon*'s workflow, as illustrated in Algorithm 1, and present a workflow visualization in Figure 1(b).

Photon assumes collaboration among multiple independent institutions, each with distinct data and compute silos, to pre-train LLMs with their own LLM-C. For enhanced data protection, the Aggregator (Agg) can be hosted by one of the institutions or a trusted third party. At the start of training, Agg initializes the model or sources it from one of the LLM-C (L.2). After initialization, Agg coordinates round information for client sampling (L.3 – 4), sends the model to each sampled client, and collects results (L.5 – 7). It then aggregates the local models to construct a new federated model (L.8 – 10), checkpointing the global model at the end of each round to enhance robustness (L.11).

At each round, sampled LLM-C instances initiate their local training pipeline by acquiring data streams from their respective private DS (L.14). For enhanced evaluation, *Photon* allows DS to use public data sources when configured. Each LLM-C evaluates available hardware resources to select the optimal execution strategy (L.15), either utilizing fast interconnection between GPUs (L.16 – 18) or applying an additional level of federated optimization if inter-GPU connectivity is limited (L.19 – 23). In the latter case, LLM-C performs an extra level of local aggregation (L.24 – 25). A local checkpoint is also maintained for quick recovery in case of failure (L.27). After completing the local training pipeline, LLM-C applies post-processing (e.g., gradient clipping, compression, or differential privacy noise injection) before returning updates to Agg (L.28).

4 *Photon* Implementation

The *Photon* implementation is highly optimized for the unique challenges of federated pre-training. Thus, it has the following objectives: (a) allow for efficient, intermittent data transfer between clients, data sources, and the aggregator; (b) effectively select the distributed training algorithm for a given client given their local GPU topology; and (c) exploit the federated communication topology to select

Algorithm 1 *Photon* execution pipeline

Require: Number of rounds T , training population P
Require: Number of clients per round K , hyperparameters H

```
1: procedure AGGREGATOR( $T, K, H, P$ )
2:    $\theta^0 \leftarrow \text{InitModel}(H)$ 
3:   for each round  $t = 1, 2, 3, \dots, T$  do
4:      $\mathcal{C} \sim \mathcal{U}(P, K)$  ▷ Sample K clients from discrete uniform distribution
5:     for  $k \in \mathcal{C}$  do in parallel
6:        $\theta_k^t, \mathcal{M}_k^t \leftarrow \text{LLM CLIENT}(k, \theta^t, H)$  ▷ Local training
7:        $\Delta_k^t \leftarrow \theta^t - \theta_k^t$  ▷ Compute model update
8:        $\Delta^t \leftarrow \frac{1}{|\mathcal{C}|} \sum_{k \in \mathcal{C}} \Delta_k^t$  ▷ Compute pseudo-gradient
9:        $\theta^{t+1} \leftarrow \text{ServerOpt}(\theta^t, -\Delta^t, t)$  ▷ Apply optimization policy on pseudo-gradient
10:       $\mathcal{M}_k^{t+1} \leftarrow \text{AggMetrics}(\mathcal{M}_k^t | \forall k \in \mathcal{C})$ 
11:      Checkpoint $(\theta_k^{t+1})$  ▷ Async checkpointing
12:   return  $\theta_k^{T+1}$ 

13: procedure LLM CLIENT( $k, \theta^t, H$ )
14:    $\mathcal{D}_k \leftarrow \text{BindStream}(k)$ 
15:    $I_k \leftarrow \text{GetNodes}(k)$ 
16:   if HasRDMA( $I_k$ ) then ▷ Check for high-bandwidth connections
17:      $B_k \leftarrow \text{CalcBatchSize}(I_k)$  ▷ Use VRAM, parameters, and sharding policy
18:      $\theta_k^t, \mathcal{M}_k^t \leftarrow \text{TrainClient}(\theta^t, \mathcal{D}_k, B_k, H)$  ▷ Use standard distributed training
19:   else ▷ Use FL as low-bandwidth training
20:     for node  $i \in I$  do in parallel
21:        $B_k^i \leftarrow \text{CalcBatchSize}(i, I_k)$ 
22:        $\mathcal{D}_k^i \leftarrow \text{PartitionStream}(i, \mathcal{D}_k)$  ▷ Apply user-set sampling policy, IID default
23:        $\theta_i^t, \mathcal{M}_i^t \leftarrow \text{TrainClient}(\theta^t, \mathcal{D}_k^i, B_k^i, H)$ 
24:        $\theta_k^t \leftarrow \frac{1}{|I|} \sum_{i \in I} \theta_i^t$  ▷ Aggregate local node models into one client update
25:        $\mathcal{M}_k^t \leftarrow \text{AggMetrics}(\mathcal{M}_i^t | \forall i \in I_k)$ 
26:   Checkpoint $(\theta_k^t, \mathcal{D}_k)$ 
27:    $\theta_k^t \leftarrow \text{PostProcess}(\theta_k^t, \mathcal{M}_k^t)$ 
28:   return  $\theta_k^t, \mathcal{M}_k^t$ 
```

the fastest aggregation method. We now discuss how our implementation, consisting of approximately 16 273 lines of code, achieves these aims.

Link between Agg and LLM-C: To enable efficient communication between Agg and LLM-C, *Photon* includes a dedicated communication module, *Link*. This module assumes a relatively fast and stable internet connection of at least 1Gbps between Agg and LLM-C, which is appropriate for the cross-silo federated setting. Serving as the communication gateway, *Link* uses secure TLS encryption and supports secure aggregation [36] for enhanced privacy, if needed. Beyond model updates, message payloads carry metadata, including training and evaluation instructions, metrics, and global instructions. *Link* provides an extensible post-processing pipeline by leveraging model compression and pruning techniques. By default, *Photon* uses lossless compression techniques without pruning.

Data Streaming for DS: Data is naturally distributed in cross-silo settings; therefore, our DS implementation breaks from the traditional one-to-one mapping between compute and data resources. Treating data as streams from one or multiple DS elements, *Photon* enables mixing arbitrary data streams with precise control over sampling across such streams. This decoupling allows data providers to operate independently of compute providers, broadening our federation. Moreover, this design reduces core network utilization if a DS can communicate with an LLM-C over a separate network. To optimize data streaming, *Photon* DS employs caching alongside optional data pre-tokenization and compression. These optimizations heuristically minimize storage overhead during the transfer from data producers to data consumers, reduce compute demands on data consumers, and maintain the throughput required by each LLM-C.

Table 1: **Computational resources of different regions.** For each region, “num. of clients x num. of GPUs held by each client” is shown, e.g., 1 x 8 H100. *Photon* enabled this globally distributed setup, overcoming challenges of low average bandwidth.

| Size | Agg | England | Utah | Texas | Quebec | Maharashtra |
|------|---------|------------|------------|------------|------------|-------------|
| 7B | England | - | 1 x 8 H100 |
| 3B | England | - | 1 x 4 H100 |
| 1B | England | 1 x 2 H100 | 2 x 2 H100 | 2 x 2 H100 | 2 x 4 H100 | 1 x 4 H100 |
| 125M | England | 2 x 1 H100 |

Optimal Training Strategy Selection for LLM-C: To accommodate the heterogeneous nature of the hardware, *Photon*’s LLM-C can support a wide range of configurations, provided the model fits within the available total VRAM with a batch size of at least one sample. An LLM-C hardware setup can include a single GPU, multiple GPUs within a server node, or multiple servers connected by high-bandwidth interconnects. *Photon* aims to maximize throughput for each LLM-C by selecting an optimal training strategy through a heuristic-based approach that is summarized as follows:

1. If a model and sufficient batch size fit within a single GPU, enabling the client to keep pace with the federation, LLM-C assigns a dedicated GPU to each client.
2. For nodes with multiple GPUs, LLM-C uses either DDP or FSDP, depending on whether a model with a viable batch size fits within a single GPU.
3. When clients have a cluster of GPU-equipped machines, LLM-C selects a strategy based on the cluster interconnection speed. High-bandwidth interconnects lead to DDP or FSDP, similar to the previous variant. In contrast, lower bandwidth may necessitate constructing sub-federations with further data sub-partitioning, with each partition trained independently.

In each case, the strategy ensures optimal compute utilization within the LLM-C topology. All LLM-C training strategies are transparent to Agg, enhancing the federation’s scalability and extensibility. Our experiments primarily use common cross-silo settings, such as allocating one GPU per client, reflecting typical institutional bandwidth constraints between servers. However, as demonstrated later, *Photon* is flexible and supports better-interconnected topologies.

Topology Between Clients: For *Photon* to efficiently pre-train an LLM in a federated setting, parameter aggregation must be effectively managed within current communication constraints. In general, a model with size $M = |\theta|$ trained across N workers can be aggregated in three variants, each with other distinct use cases, advantages, and limitations:

1. A *parameter server* (PS) receives all updates from participating workers. This variant is ideal for relatively small N , as the data received by the server scales in $\mathcal{O}(NM)$. It handles worker dropouts well by providing a partial update derived from surviving workers and is the only viable option when privacy restrictions prohibit peer-to-peer communication.
2. Workers communicate directly via *AllReduce* (AR). In this setup, each worker sends its model to all peers and receives models from all others, resulting in $\mathcal{O}(N^2M)$ data transmission per worker. Like PS, AllReduce tolerates dropouts well, enabling partial updates from remaining workers; however, privacy limitations may restrict peer-to-peer communication.
3. Workers use *Ring-AllReduce* (RAR), communicating over a ring topology for efficient aggregation. This bandwidth-optimal method requires each worker to send/receive $\mathcal{O}(M)$ data, with the bottleneck being the slowest link in the ring. RAR does not tolerate dropouts and has similar privacy considerations to AllReduce.

Each method has its constraints, and *Photon* adapts to select the most efficient option for each scenario.

5 Evaluation

This section demonstrates the effectiveness of *Photon* in training large language models (LLMs) from scratch in federated settings, compared to models trained using standard centralized methods and prior low-bandwidth distributed approaches. We evaluate models based on final performance, compute efficiency, and communication scalability.



Figure 2: **The locations and bandwidth of participating clients in the Federation**, with multiple nodes equipped with H100s at each site. More details are available in Table 1. Bandwidth between regions varies significantly, impacting the efficiency of *Photon*'s aggregation procedures. The map shows the RAR topology (gray dashed line) and the PS topology (black solid line). The slowest link in the RAR topology, between Maharashtra and Quebec, acts as a bottleneck. In the PS topology, the connection speed to England limits each update's communication.

5.1 Experimental Setup

Our experiments employ a cross-silo FL setup where clients are equipped with one or more high-end GPUs, such as Nvidia H100s, and are interconnected via the Internet. The computational resources used on each client vary based on model size: million-parameter models are trained using a single GPU, whereas billion-scale models may require up to 8 GPUs per client. We present the five locations used during training for our distributed setup in Fig. 2, with details on the number of clients and GPUs available per client provided in Table 1.

The client's local batch size is determined by its VRAM, model size, and optimal throughput, leveraging heuristics similar to those proposed by the Microsoft DeepSpeed AutoTuner [37, 38]. For instance, clients training a 125M parameter model use 1 Nvidia H100, processing a hardware-determined local batch size $B_l = 32$, without gradient accumulation or activation checkpointing, to maximize throughput. Given the assumption of homogeneous client resources, all clients independently employ the same local throughput optimization strategies. Experiments are conducted using PyTorch (v2.4.0) with mixed precision context `bf16` (BF16). The model architecture is based on the MPT (Mosaic Pre-Trained) family of decoder-only transformers [39], with the MPT centralized training recipe used as a baseline configuration.

Datasets and Training Recipe. We model data distribution across clients by randomly partitioning the C4 [40] dataset uniformly into 64 equally sized shards. N clients, hence, refer to a subset of N shards from these 64 shards. The local training step for clients uses AdamW [41] as the optimizer, with a cosine learning rate schedule and an initial linear warm-up phase. We report all hyperparameters in Appendix A. The learning rate schedule varies by model size and is adjusted to match the batch size and total token count seen in centralized training. We experiment with different numbers of local steps per round, specifically $\{62, 128, 512\}$, which defines the amount of local work done by clients. Model performance is evaluated using perplexity on the full C4 validation set.

To explore the robustness of *Photon* to data heterogeneity, we also explore a setting where clients hold data from a variety of text sources representing diverse categories. Specifically, we use The Pile [42] dataset, which includes text sources from ArXiv (academic), C4 and Wikipedia (internet), and Project Gutenberg (prose) to capture a range of language styles while providing sufficient data for scaling. For our experiments with full participation, we explore three configurations: four clients (one text source per client), eight clients (two text sources split into two clients), and sixteen clients (four text sources split into four clients). For partial participation, we adopt the sixteen-client configuration, sampling 25%, 50%, and 100% of clients per round, with evaluation on C4.

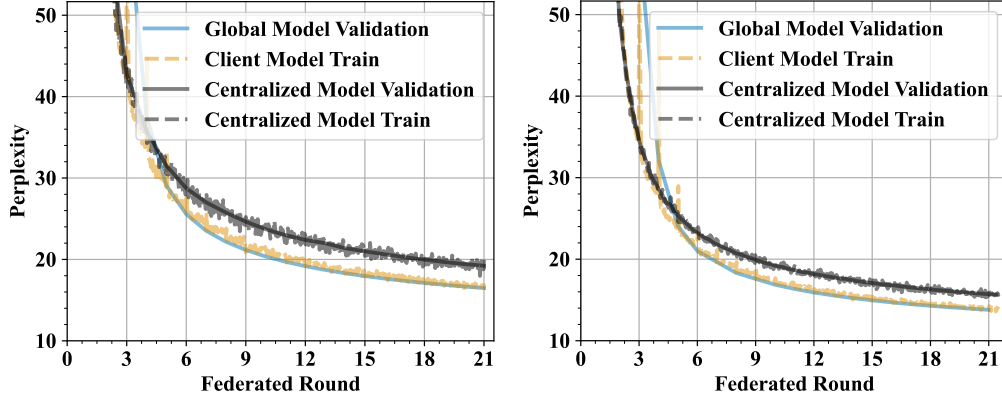


Figure 3: **Comparison of perplexity convergence (lower is better) for Photon and centralized training with 3B (top) and 7B (bottom) models.** The federated global model was evaluated on the C4 test set, with averaged train perplexities across clients and centralized train/test perplexities presented for both models. These large federated models show lower perplexity than centralized models and remain stable during aggregation, with minimal perplexity spikes after early rounds.

5.2 Photon trains Billion-sized LLMs

Using *Photon*, we train models up to 7B parameters from scratch in federations of 16 to 4 clients, using full participation every round and prove they outperform their centralized counterparts. While previous results suggest that federated optimization is generally inferior to standard SGD in terms of loss [25] and that LLM pre-training may be less sample-efficient [9, 14], we find it to be quite competitive in terms of wall-clock time and, comparable if not slightly superior in terms of loss. As shown in Figs. 3 and 4, the 3B and 7B models achieve 13.8% to 16.9% lower perplexity than models trained using centralized training. As shown in Table 2, such models outperform in terms of perplexity whilst being efficient to train in distributed settings. For instance, when utilizing identical computational resources with a 10 Gbps connection and Ring-AllReduce, Table 2 demonstrates that federated optimization for the 7B model to reach the same perplexity requires only 95.6 total hours of training due to 500x less frequent communication, whereas centralized methods require over 147 hours. Higher-bandwidth connections such as InfiniBand would bring the total time closer to the compute time. Moving beyond perplexity, we also show that the models produced by *Photon* are effective for downstream tasks in Appendix D.1.

We observe that the perplexity gap between federated and centralized models widens at larger scales; smaller models converge to similar performance levels across methods. Additionally, as model size grows, training stability improves, as we observe perplexity spikes decreasing in magnitude compared to smaller models. Our observed performance improvements stem from the noise-injecting [24] and meta-learning [34] of our federated optimization. As we will later see, federated optimization supports high learning rates with small batch sizes, enhancing generalization via noise injection [35].

Figure 4: **Our results show federated models to be comparable to centralized and potentially superior as they obtain lower perplexity (PP) given the same computational resources.** Their perplexity gains grow with model size.

| Size | Fed PP | Cent PP | Gain (%) |
|------|--------|---------|----------|
| 1.3B | 20.1 | 23.2 | 13.4% |
| 3B | 15.7 | 18.2 | 13.7% |
| 7B | 13.8 | 16.6 | 16.9% |

5.3 Photon Model Performance Scales with Federation Size

Previous works [43, 9] raised concerns about the wall time benefits of increasing the federated population size. Using *Photon*, we show that client contributions to the global model convergence depend on the amount of local work, based on the following hyperparameters: the number of local training steps per round and the global batch size $B_g = NB_l \in \{32, 64, 128, 256, 512\}$, where $N \in \{1, 2, 4, 8, 16\}$ is the number of clients per round, and $B_l = 32$ is the local batch size.

Table 2: We report system metrics for the billion-scale models trained with *Photon* and their centralized baselines, including total wall time with compute and communication time breakdowns. We provide GPU efficiency metrics such as average GPU utilization and Model FLOPs Utilization (MFU) during local computation. *Photon*’s federated approach shortens training time by reducing communication steps, assuming consistent setups: the number of federated clients matches data-parallel workers, aggregation uses *Ring-AllReduce* with a fixed 10Gbps bandwidth for the slowest link, and both clients and workers maintain the same mini-batch throughput.

| Model | Wall Time [h] | Compute Time [h] | Comm. Time [h] | Local Util. GPU [%] | Local MFU per device |
|----------|---------------|------------------|----------------|---------------------|----------------------|
| Cen-1.3B | 26.7 (1×) | 6.5 (1×) | 20.2 (1×) | 74 | 0.8027 |
| Fed-1.3B | 18.02 (0.67×) | 18.0 (2.8×) | 0.02 (0.001×) | 83 | 1.1245 |
| Cen-3B | 56.6 (1×) | 16.1 (1×) | 40.48 (1×) | 81 | 0.165 |
| Fed-3B | 25.2 (0.45×) | 25.1 (1.6×) | 0.05 (0.001×) | 78 | 0.240 |
| Cen-7B | 147.9 (1×) | 50.7 (1×) | 97.2 (1×) | 88 | 0.335 |
| Fed-7B | 95.6 (0.65×) | 95.5 (1.9×) | 0.1 (0.001×) | 90 | 0.224 |

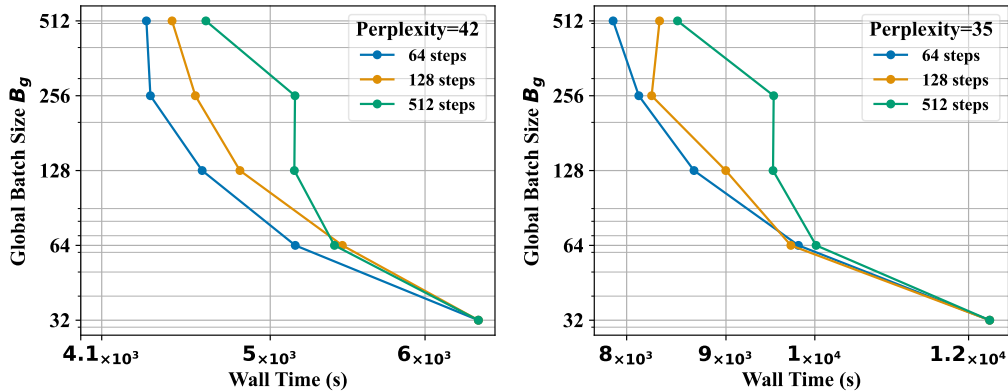


Figure 5: The tradeoff between time and compute resources (the larger batch size, the more resources) spent to train a model by *Photon* to target perplexities (top 42 and bottom 35). We measure the impact of the global batch size $B_g = NB_l$, where $N \in \{1, 2, 4, 8, 16\}$ (number of clients per round) and $B_l = 32$ (local batch size), on the wall time needed to reach two target perplexities: 42 (top, near the centralized baseline) and 35 (bottom, near optimum). Fewer local steps per round (64) show clear benefits from increasing B_g for both perplexity targets, but with more local work (128 and 512 steps), the returns on reduced wall time diminish.

As illustrated in Figure 5, more frequent communication (smaller local steps per round) leads to greater wall time reductions with larger B_g . The trends are smoother for a higher target perplexity of 42 than at a lower target perplexity. On the other hand, at a target perplexity of 35, the gains in wall time drop as B_g increases, especially at 128 steps per round. This phenomenon is also observed in McCandlish et al. [44], where increasing the batch size in the centralized setting led to diminishing returns in wall time. For more details, see Appendix C.1. Hence, depending on the target perplexity and local steps per round, a compute-optimal regime exists where the global batch size B_g must be carefully tuned to maximize the number of available clients.

Comparison with State-of-the-Art. Through utilizing the aforementioned compute-optimal regime, *Photon* significantly outperforms previous state-of-the-art LLM distributed pre-training framework, DiLoCo [9]. In Table 3, we train a model with 125M parameters, varying the number of clients $N \in \{2, 4, 8\}$, and using a local batch size $B_l = 32$. We show that, within an appropriate global batch size B_g regime, DiLoCo yields limited returns as the number of clients per round increases and requires roughly 2× more time to reach the same perplexity for both target values, 42 and 35. We observe similar trends across different B_g settings used in DiLoCo.

In Douillard et al. [9], the authors adopted a much higher compute regime. DiLoCo trains a *smaller* model (75M parameter) with $B_l = 512$, $N = 8$, and $B_g = 4096$ for 88 000 steps, which corresponds

Table 3: *Photon* consistently reaches a satisfactory perplexity twice as fast as DiLoCo ($\eta = 0.1$) across three client counts. We evaluated the impact of the global batch size $B_g = NB_l$, where $N \in \{2, 4, 8\}$ (clients per round) and $B_l = 32$ (local batch size), on the wall time required to reach target perplexities of 42 (near the centralized baseline) and 35 (near optimal). Results show the wall time gap between *Photon* and DiLoCo when tuning the server learning rate $\eta_s = 0.1$ to meet the target perplexities.

| N | Method | Wall Time [s] | |
|-----|---------------------------|-------------------------|--------------------------|
| | | PPL = 42 | PPL = 35 |
| 2 | DiLoCo ($\eta_s = 0.1$) | 10528.8 (1 \times) | 19516.8 (1 \times) |
| | <i>Photon</i> | 5392.8 (0.51 \times) | 10015.2 (0.51 \times) |
| 4 | DiLoCo ($\eta_s = 0.1$) | 10545.2 (1 \times) | 19032.8 (1 \times) |
| | <i>Photon</i> | 5144.0 (0.49 \times) | 9516.4 (0.5 \times) |
| 8 | DiLoCo ($\eta_s = 0.1$) | 9523.8 (1 \times) | 20334.6 (1 \times) |
| | <i>Photon</i> | 5148.0 (0.54 \times) | 9523.8 (0.47 \times) |

to 46B tokens per worker and 369B tokens in total, far beyond the compute-optimal 1.5B estimated by Hoffmann et al. [45]¹. In contrast, for the **larger** 125M model, *Photon* automatically tunes the local batch size $B_l = 32$ to suit the hardware capabilities and achieve 9000 cumulative training steps per client when using four clients per round, reaching 2.32B token processed in total, close to the compute-optimal 2.5B tokens estimated by Hoffmann et al. [45].

5.4 *Photon*'s Comms. Efficiency and Scalability

Communication is an overhead in FL, often scaling poorly as the number of clients grows. In this section, we evaluate the communication scalability of *Photon*, considering its nontrivial relationship with the faster convergence speed brought by using more clients per round (Fig. 5). Thus, we examine three aggregation implementations for *Photon*: *parameter server* (PS), *AllReduce* (AR), and *Ring-AllReduce* (RAR). These approaches are detailed in Section 4.

Increasing the number of clients per round speeds up convergence, reducing the required communication steps. Thus, we evaluate communication scalability by varying the number of clients per round, $N \in \{2, 4, 8, 16\}$ (excluding $N = 1$, as no communication occurs). Since the number of pseudo-gradients communicated and aggregated scales linearly with the number of clients and model size, we use the most communication-efficient setup in our experiments. Specifically, clients perform 512 local steps per round, training a 125M parameter model targeting a perplexity of 35.

Figure 6 shows that communication overhead increases with N , especially under the PS implementation due to its limited scalability. However, using more clients accelerates convergence, reducing the required communication steps and mitigating the costlier communication. Except at the largest cohort size (16 clients), the less

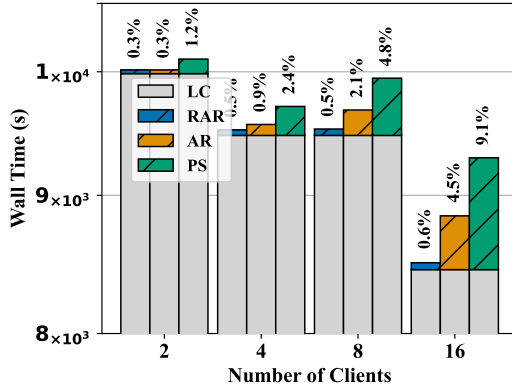


Figure 6: **Wall time comparison among different topologies.** We report total wall time divided into local compute (LC) and communication time. Communication time is evaluated for three aggregation methods: *parameter server* (PS) for privacy-constrained settings, *AllReduce* (AR) for better scalability, and *Ring-AllReduce* (RAR), the most scalable but limited by the slowest link. As expected, communication costs rise with more clients. However, efficient implementations like RAR maintain the wall time reduction from scaling compute resources. The top indicates the percentage of time spent on communication for each method.

¹The original work is not explicit if 512 is global or local. Substituting $B_l = \frac{512}{8}$ gives similar conclusions, with 5.75B tokens per worker and 46B in total, far beyond the optimal 1.5B.

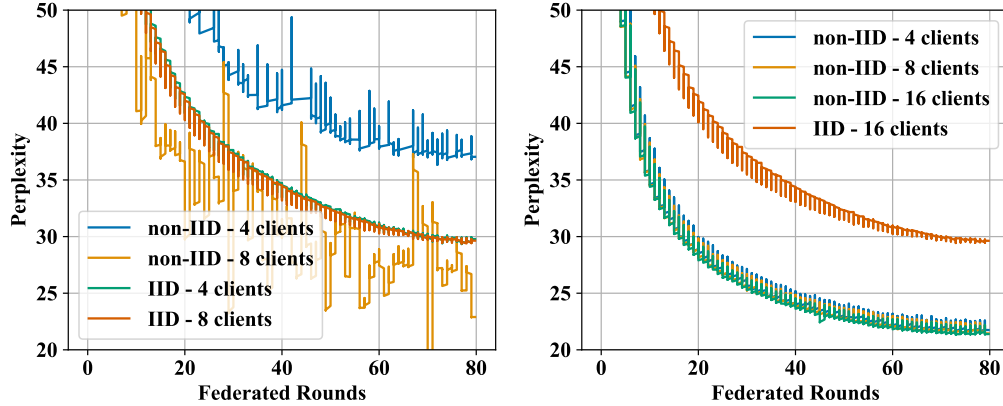


Figure 7: We assess *Photon*’s robustness to data heterogeneity by training with (top) and without (bottom) partial participation. Federation of clients using data from The Pile dataset, as described in Section 5.1. Results from homogeneous data distribution (IID) experiments for reference. While partial participation causes larger fluctuations across rounds, full participation behaves similarly to the IID case. In all settings, increasing the number of clients per round accelerates achieving the target perplexity, with the effect more pronounced under partial participation.

scalable implementations (PS and AR) account for a minor portion of wall time relative to the local computation (LC) time at clients. Figure 6 highlights RAR as the most scalable option when minimizing communication time is crucial.

5.5 *Photon*’s Robustness to Data Heterogeneity

In typical federated learning scenarios, clients possess heterogeneous data distributions, raising concerns about the robustness of federated optimization. Non-coherent pseudo-gradient updates across clients can impact model convergence by slowing it down or reducing performance. This challenge is compounded by privacy restrictions that prevent observing client data distributions directly.

We assess *Photon*’s robustness to data heterogeneity by training on different data sources from The Pile dataset, distributed across clients as described in Section 5.1. The most challenging scenario involves partial participation of the client population, where the global federated model is only intermittently exposed to diverse data distributions. Figure 7 (top) shows that higher client sampling ratios improve convergence speed, final performance, and convergence smoothness under partial participation, demonstrating *Photon*’s robustness to heterogeneous data.

Under full participation, Figure 7 (bottom) indicates that larger client cohorts reduce wall-clock training time, though less effectively than with IID data due to conflicting gradients from diverse sources [43]. Aggregation methods designed for heterogeneous data, as in [46], could further enhance convergence in such cases.

6 Opportunities and Limitations

Our proposed *Photon* introduces both algorithmic and system optimization techniques to achieve state-of-the-art LLM pre-training across distributed heterogeneous data. In this section, we reiterate some of our work’s limitations and expand on some of our research’s potential opportunities and applications.

Federated Hyperparameter Tuning. In Section 5.3, we emphasize the importance of selecting the global batch size to maximize computational resources and performance. A natural extension of our work would be to investigate other critical hyperparameters, such as the learning rate, learning rate scheduler, and their interaction with batch size. *Photon*’s significant reduction in pre-training costs for LLMs makes it feasible to leverage existing federated hyperparameter optimization algorithms [47, 48] to explore optimal global or per-client hyperparameters.

Addressing Data Heterogeneity. Our experiments in Section 5.5 demonstrate *Photon*’s robustness in handling data heterogeneity. However, further exploration of alternative aggregation strategies, loss functions, and client selection methods could enhance performance under such conditions. Techniques include minimizing the Euclidean distance or maximizing agreement between global and local models [49, 50], reducing local model divergence from the global model [51, 52], and measuring client contributions [53, 54], with client selection based on their value to the global model [55, 56]. Most of these methods can be directly integrated into *Photon*.

Continual Pre-training & Personalization. A key advantage of using *Photon* for pre-training LLMs is improved model convergence and performance, offering a stronger initialization for continual pre-training or personalization. This aligns with findings from previous studies [57, 58], which highlight the importance of starting with a strong pre-trained model to stabilize federated training and enhance global model performance. A robust pre-trained model also benefits LLM personalization by enabling further fine-tuning or per-client learning strategies [59].

Cross-device Federated Scenarios. In this work, we demonstrate how *Photon* effectively addresses the challenges of cross-silo FL. Another common context is cross-device FL, where clients are often lower-compute devices like mobile phones and IoT devices. To handle the diverse system heterogeneity in these scenarios, *Photon* can be extended with existing methods proven successful in cross-device FL, such as parameter-efficient fine-tuning [60, 61], quantization [62], low-rank decomposition [63], pruning [64, 65], and early exits [66–68].

7 Related Work

Recent advances in large-scale FL and distributed deep learning focus on improving scalability, efficiency, and privacy while addressing challenges like device heterogeneity and system constraints. Early efforts, such as [69], emphasize system design in FL for mobile devices, addressing resource limitations and connectivity in applications like Google’s Gboard. Asynchronous FL systems like PAPAYA [70] improve scalability by allowing clients to update models independently, boosting convergence speed and reducing communication overhead. Platforms like FLINT [71] simulate real-world FL constraints, benefiting large-scale applications like LinkedIn. In distributed deep learning, PyTorch’s Fully Sharded Data Parallel (FSDP) [72] and Distributed Data Parallel (DDP) [73] are crucial for scalable training, while frameworks like Horovod [21] use *Ring-AllReduce* to simplify distributed learning. Tools like Dataset Grouper [74] help create large-scale datasets, and systems like MAST [3] optimize workload placement across data centers. ZeRO [75–77] and PETALS [78, 79] extend scalability, enabling training and inference for models with trillions of parameters and decentralized deployment, respectively, providing robust solutions for large-scale ML.

In federated or collaborative LLM training, most efforts have focused on fine-tuning [80, 81] or inference [78, 79], with pre-training only recently gaining attention [9, 14, 16]. Previously, federated learning primarily centered on cross-device settings, which are unsuited to pre-training’s substantial hardware demands. Douillard et al. [9], discussed in the main work, achieves notable communication reductions in a high-compute training regime. Sani et al. [14] introduces a library for LLM pre-training and provides initial results on large models. Nous Research [16] offers early findings on a peer-to-peer AllReduce approach to Federated Learning.

8 Conclusion

This work introduces *Photon*, the first federated system for decentralized end-to-end LLM pre-training in low-bandwidth, globally distributed settings. *Photon* enables collaborative training of models up to 7B parameters, outperforming centralized training in perplexity. By pooling client resources, *Photon* accelerates training as compute scales, and in low-bandwidth conditions, it surpasses standard distributed training by increasing throughput and reducing communication costs. This is achieved through adaptive local parallelism, which dynamically switches between distributed algorithms and low-bandwidth Local SGD based on client connectivity. With small local batch sizes and high learning rates, *Photon* supports an aggressive training strategy, making it the first cost-effective solution to scale LLM pre-training beyond data centers.

Acknowledgments and Disclosure of Funding

All costs for the computation used for this work was funded by Flower Labs, and the research conducted by a team of researchers from Flower Labs and The University of Cambridge. Support for university based researchers came from a variety of sources, but in particular the following funding organizations are acknowledged: the European Research Council (REDIAL), the Royal Academy of Engineering (DANTE) and the Ministry of Education of Romania through the Credit and Scholarship Agency.

References

- [1] Jared Kaplan, Sam McCandlish, Tom Henighan, Tom B Brown, Benjamin Chess, Rewon Child, Scott Gray, Alec Radford, Jeffrey Wu, and Dario Amodei. Scaling laws for neural language models. *arXiv preprint arXiv:2001.08361*, 2020.
- [2] Ziheng Jiang, Haibin Lin, Yinmin Zhong, Qi Huang, Yangrui Chen, Zhi Zhang, Yanghua Peng, Xiang Li, Cong Xie, Shibiao Nong, Yulu Jia, Sun He, Hongmin Chen, Zhihao Bai, Qi Hou, Shipeng Yan, Ding Zhou, Yiyao Sheng, Zhuo Jiang, Haohan Xu, Haoran Wei, Zhang Zhang, Pengfei Nie, Leqi Zou, Sida Zhao, Liang Xiang, Zherui Liu, Zhe Li, Xiaoying Jia, Jianxi Ye, Xin Jin, and Xin Liu. Megascale: Scaling large language model training to more than 10, 000 gpus. In *21st USENIX Symposium on Networked Systems Design and Implementation, NSDI 2024*, pages 745–760. USENIX Association, 2024.
- [3] Arnab Choudhury, Yang Wang, Tuomas Pelkonen, Kutta Srinivasan, Abha Jain, Shenghao Lin, Delia David, Siavash Soleimanifard, Michael Chen, Abhishek Yadav, Ritesh Tijoriwala, Denis Samoylov, and Chunqiang Tang. MAST: global scheduling of ML training across geodistributed datacenters at hyperscale. In *18th USENIX Symposium on Operating Systems Design and Implementation, OSDI 2024*, pages 563–580. USENIX Association, 2024.
- [4] Jeff Rasley, Samyam Rajbhandari, Olatunji Ruwase, and Yuxiong He. Deepspeed: System optimizations enable training deep learning models with over 100 billion parameters. In *Proceedings of the 26th ACM SIGKDD International Conference on Knowledge Discovery & Data Mining, KDD '20*, page 3505–3506. Association for Computing Machinery, 2020. ISBN 9781450379984. doi: 10.1145/3394486.3406703.
- [5] Kevin Lee, Adi Gangidi, and Mathew Oldham. Building Meta’s GenAI infrastructure, March 2024. Categories: AI Research, Data Center Engineering, ML Applications.
- [6] Kun Qian, Yongqing Xi, Jiamin Cao, Jiaqi Gao, Yichi Xu, Yu Guan, Binzhang Fu, Xuemei Shi, Fangbo Zhu, Rui Miao, Chao Wang, Peng Wang, Pengcheng Zhang, Xianlong Zeng, Eddie Ruan, Zhiping Yao, Ennan Zhai, and Dennis Cai. Alibaba HPN: A data center network for large language model training. In *Proceedings of the ACM SIGCOMM 2024 Conference, ACM SIGCOMM 2024, Sydney, NSW, Australia, August 4-8, 2024*, pages 691–706. ACM, 2024. doi: 10.1145/3651890.3672265.
- [7] Qinghao Hu, Zhisheng Ye, Zerui Wang, Guoteng Wang, Meng Zhang, Qiaoling Chen, Peng Sun, Dahua Lin, Xiaolin Wang, Yingwei Luo, Yonggang Wen, and Tianwei Zhang. Characterization of large language model development in the datacenter. In *21st USENIX Symposium on Networked Systems Design and Implementation (NSDI 24)*, pages 709–729. USENIX Association, 2024. ISBN 978-1-939133-39-7.
- [8] Fei Yang, Shuang Peng, Ning Sun, Fangyu Wang, Yuanyuan Wang, Fu Wu, Jiezhong Qiu, and Aimin Pan. Holmes: Towards distributed training across clusters with heterogeneous NIC environment. In *Proceedings of the 53rd International Conference on Parallel Processing ICPP 2024*, pages 514–523. ACM, 2024.
- [9] Arthur Douillard, Qixuang Feng, Andrei A. Rusu, Rachita Chhaparia, Yani Donchev, Adhiguna Kuncoro, Marc’Aurelio Ranzato, Arthur Szlam, and Jiajun Shen. Diloco: Distributed low-communication training of language models. *CoRR*, abs/2311.08105, 2023. doi: 10.48550/ARXIV.2311.08105.

- [10] Zhenheng Tang, Xueze Kang, Yiming Yin, Xinglin Pan, Yuxin Wang, Xin He, Qiang Wang, Rongfei Zeng, Kaiyong Zhao, Shaohuai Shi, et al. Fusionllm: A decentralized llm training system on geo-distributed gpus with adaptive compression. *arXiv preprint arXiv:2410.12707*, 2024.
- [11] Alexander Borzunov, Max Ryabinin, Artem Chumachenko, Dmitry Baranchuk, Tim Dettmers, Younes Belkada, Pavel Samygin, and Colin A Raffel. Distributed inference and fine-tuning of large language models over the internet. *Conference on Neural Information Processing Systems*, 36, 2024.
- [12] Haibo Mi, Kele Xu, Dawei Feng, Huaimin Wang, Yiming Zhang, Zibin Zheng, Chuan Chen, and Xu Lan. Collaborative deep learning across multiple data centers. *Sci. China Inf. Sci.*, 63(8):1–11, 2020.
- [13] Q Chang, Z Yan, M Zhou, et al. Mining multi-center heterogeneous medical data with distributed synthetic learning. *Nature Communications*, 14(5510):5510, 2023. doi: 10.1038/s41467-023-40687-y.
- [14] Lorenzo Sani, Alex Jacob, Zeyu Cao, Bill Marino, Yan Gao, Tomas Paulik, Wanru Zhao, William F Shen, Preslav Aleksandrov, Xinchu Qiu, et al. The future of large language model pre-training is federated. *arXiv preprint arXiv:2405.10853*, 2024.
- [15] Brendan McMahan, Eider Moore, Daniel Ramage, Seth Hampson, and Blaise Agüera y Arcas. Communication-efficient learning of deep networks from decentralized data. In *Artificial intelligence and statistics*. PMLR, 2017.
- [16] Nous Research. DisTrO, 2024. URL https://github.com/NousResearch/DisTrO/blob/main/A_Preliminary_Report_on_DisTrO.pdf.
- [17] Qiaozhi He, Xiaomin Zhuang, and Zhihua Wu. Exploring scaling laws for local sgd in large language model training. *arXiv preprint arXiv:2409.13198*, 2024.
- [18] Othmane Marfoq, Chuan Xu, Giovanni Neglia, and Richard Vidal. Throughput-optimal topology design for cross-silo federated learning. *Advances in Neural Information Processing Systems*, 33:19478–19487, 2020.
- [19] Sebastian U. Stich. Local SGD converges fast and communicates little. In *International Conference on Learning Representations*, 2019.
- [20] Mengwei Xu, Dongqi Cai, Yaozong Wu, Xiang Li, and Shangguang Wang. {FwdLLM}: Efficient federated finetuning of large language models with perturbed inferences. In *2024 USENIX Annual Technical Conference (USENIX ATC 24)*, pages 579–596, 2024.
- [21] Alexander Sergeev and Mike Del Balso. Horovod: fast and easy distributed deep learning in tensorflow. *CoRR*, abs/1802.05799, 2018.
- [22] Peter Kairouz, H. Brendan McMahan, Brendan Avent, Aurélien Bellet, Mehdi Bennis, Arjun Nitin Bhagoji, Kallista A. Bonawitz, Zachary Charles, Graham Cormode, Rachel Cummings, Rafael G. L. D’Oliveira, Hubert Eichner, Salim El Rouayheb, David Evans, Josh Gardner, Zachary Garrett, Adrià Gascón, Badih Ghazi, Phillip B. Gibbons, Marco Gruteser, Zaïd Harchaoui, Chaoyang He, Lie He, Zhouyuan Huo, Ben Hutchinson, Justin Hsu, Martin Jaggi, Tara Javidi, Gauri Joshi, Mikhail Khodak, Jakub Konečný, Aleksandra Korolova, Farinaz Koushanfar, Sanmi Koyejo, Tancrede Lepoint, Yang Liu, Prateek Mittal, Mehryar Mohri, Richard Nock, Ayfer Özgür, Rasmus Pagh, Hang Qi, Daniel Ramage, Ramesh Raskar, Mariana Raykova, Dawn Song, Weikang Song, Sebastian U. Stich, Ziteng Sun, Ananda Theertha Suresh, Florian Tramèr, Praneeth Vepakomma, Jianyu Wang, Li Xiong, Zheng Xu, Qiang Yang, Felix X. Yu, Han Yu, and Sen Zhao. Advances and open problems in federated learning. *Found. Trends Mach. Learn.*, 14(1-2):1–210, 2021. doi: 10.1561/22000000083.
- [23] Jose Javier Gonzalez Ortiz, Jonathan Frankle, Mike Rabbat, Ari S. Morcos, and Nicolas Ballas. Trade-offs of local SGD at scale: An empirical study. *CoRR*, abs/2110.08133, 2021.
- [24] Tao Lin, Sebastian U. Stich, Kumar Kshitij Patel, and Martin Jaggi. Don’t use large mini-batches, use local SGD. In *International Conference on Learning Representations*, 2020.

- [25] Jianyu Wang, Zachary Charles, Zheng Xu, Gauri Joshi, H. Brendan McMahan, Blaise Agüera y Arcas, Maruan Al-Shedivat, Galen Andrew, Salman Avestimehr, Katharine Daly, Deepesh Data, Suhas N. Diggavi, Hubert Eichner, Advait Gadhihar, Zachary Garrett, Antonious M. Girgis, Filip Hanzely, Andrew Hard, Chaoyang He, Samuel Horváth, Zhouyuan Huo, Alex Ingerman, Martin Jaggi, Tara Javidi, Peter Kairouz, Satyen Kale, Sai Praneeth Karimireddy, Jakub Konečný, Sanmi Koyejo, Tian Li, Luyang Liu, Mehryar Mohri, Hang Qi, Sashank J. Reddi, Peter Richtárik, Karan Singhal, Virginia Smith, Mahdi Soltanolkotabi, Weikang Song, Ananda Theertha Suresh, Sebastian U. Stich, Ameet Talwalkar, Hongyi Wang, Blake E. Woodworth, Shanshan Wu, Felix X. Yu, Honglin Yuan, Manzil Zaheer, Mi Zhang, Tong Zhang, Chunxiang Zheng, Chen Zhu, and Wennan Zhu. A field guide to federated optimization. *CoRR*, abs/2107.06917, 2021.
- [26] Jordan Hoffmann, Sebastian Borgeaud, Arthur Mensch, Elena Buchatskaya, Trevor Cai, Eliza Rutherford, Diego de Las Casas, Lisa Anne Hendricks, Johannes Welbl, Aidan Clark, Thomas Hennigan, Eric Noland, Katherine Millican, George van den Driessche, Bogdan Damoc, Aurelia Guy, Simon Osindero, Karén Simonyan, Erich Elsen, Oriol Vinyals, Jack Rae, and Laurent Sifre. An empirical analysis of compute-optimal large language model training. In *Conference on Neural Information Processing Systems*, volume 35, pages 30016–30030, 2022.
- [27] Jeffrey Dean, Greg Corrado, Rajat Monga, Kai Chen, Matthieu Devin, Mark Mao, Marc' aurelio Ranzato, Andrew Senior, Paul Tucker, Ke Yang, Quoc Le, and Andrew Ng. Large scale distributed deep networks. In *Advances in Neural Information Processing Systems*, volume 25. Curran Associates, Inc., 2012.
- [28] Deepak Narayanan, Aaron Harlap, Amar Phanishayee, Vivek Seshadri, Nikhil R. Devanur, Gregory R. Ganger, Phillip B. Gibbons, and Matei Zaharia. Pipedream: generalized pipeline parallelism for dnn training. In *Proceedings of the 27th ACM Symposium on Operating Systems Principles, SOSP '19*, page 1–15, New York, NY, USA, 2019. Association for Computing Machinery. ISBN 9781450368735. doi: 10.1145/3341301.3359646.
- [29] Deepak Narayanan, Mohammad Shoeybi, Jared Casper, Patrick LeGresley, Mostofa Patwary, Vijay Korthikanti, Dmitri Vainbrand, Prethvi Kashinkunti, Julie Bernauer, Bryan Catanzaro, Amar Phanishayee, and Matei Zaharia. Efficient large-scale language model training on gpu clusters using megatron-lm. In *Proceedings of the International Conference for High Performance Computing, Networking, Storage and Analysis, SC '21*, New York, NY, USA, 2021. Association for Computing Machinery. ISBN 9781450384421. doi: 10.1145/3458817.3476209.
- [30] Alexander Sergeev and Mike Del Balso. Horovod: fast and easy distributed deep learning in tensorflow. *arXiv preprint arXiv:1802.05799*, 2018.
- [31] Adithya Gangidi, Rui Miao, Shengbao Zheng, Sai Jayesh Bondu, Guilherme Goes, Hany Morsy, Rohit Puri, Mohammad Riftadi, Ashmitha Jeevaraj Shetty, Jingyi Yang, Shuqiang Zhang, Mikel Jimenez Fernandez, Shashidhar Gandham, and Hongyi Zeng. Rdma over ethernet for distributed training at meta scale. In *Proceedings of the ACM SIGCOMM 2024 Conference, ACM SIGCOMM '24*, page 57–70, New York, NY, USA, 2024. Association for Computing Machinery. ISBN 9798400706141. doi: 10.1145/3651890.3672233.
- [32] Wenxue Li, Xiangzhou Liu, Yuxuan Li, Yilun Jin, Han Tian, Zhizhen Zhong, Guyue Liu, Ying Zhang, and Kai Chen. Understanding communication characteristics of distributed training. In *Proceedings of the 8th Asia-Pacific Workshop on Networking, APNet '24*, page 1–8, New York, NY, USA, 2024. Association for Computing Machinery. ISBN 9798400717581. doi: 10.1145/3663408.3663409.
- [33] Sunwoo Lee, Qiao Kang, Ankit Agrawal, Alok Choudhary, and Wei-keng Liao. Communication-efficient local stochastic gradient descent for scalable deep learning. In *2020 IEEE International Conference on Big Data (Big Data)*, pages 718–727, 2020. doi: 10.1109/BigData50022.2020.9378178.
- [34] A Nichol. On first-order meta-learning algorithms. *arXiv preprint arXiv:1803.02999*, 2018.
- [35] Nitish Shirish Keskar, Dheevatsa Mudigere, Jorge Nocedal, Mikhail Smelyanskiy, and Ping Tak Peter Tang. On large-batch training for deep learning: Generalization gap and sharp minima. In *International Conference on Learning Representations*, 2017.

- [36] Keith Bonawitz, Vladimir Ivanov, Ben Kreuter, Antonio Marcedone, H Brendan McMahan, Sarvar Patel, Daniel Ramage, Aaron Segal, and Karn Seth. Practical secure aggregation for federated learning on user-held data. *arXiv preprint arXiv:1611.04482*, 2016.
- [37] Microsoft DeepSpeed Team. Microsoft DeepSpeed, 2024. URL <https://www.deepspeed.ai/>.
- [38] Microsoft DeepSpeed Team. DeepSpeed Autotuning, 2024. URL <https://github.com/microsoft/DeepSpeed/tree/master/deepspeed/autotuning>.
- [39] MosaicML NLP Team. Introducing MPT-7B: A New Standard for Open-Source, Commercially Usable LLMs, 2023. URL <https://www.databricks.com/blog/mpt-7b>.
- [40] Colin Raffel, Noam Shazeer, Adam Roberts, Katherine Lee, Sharan Narang, Michael Matena, Yanqi Zhou, Wei Li, and Peter J. Liu. Exploring the limits of transfer learning with a unified text-to-text transformer. *J. Mach. Learn. Res.*, 21:140:1–140:67, 2020.
- [41] Ilya Loshchilov and Frank Hutter. Decoupled weight decay regularization. In *International Conference on Learning Representations*, 2019.
- [42] Leo Gao, Stella Biderman, Sid Black, Laurence Golding, Travis Hoppe, Charles Foster, Jason Phang, Horace He, Anish Thite, Noa Nabeshima, et al. The pile: An 800gb dataset of diverse text for language modeling. *arXiv preprint arXiv:2101.00027*, 2020.
- [43] Zachary Charles, Zachary Garrett, Zhouyuan Huo, Sergei Shmulyian, and Virginia Smith. On large-cohort training for federated learning. In *Conference on Neural Information Processing Systems*, pages 20461–20475, 2021.
- [44] Sam McCandlish, Jared Kaplan, Dario Amodei, and OpenAI Dota Team. An empirical model of large-batch training. *CoRR*, abs/1812.06162, 2018.
- [45] Jordan Hoffmann, Sebastian Borgeaud, Arthur Mensch, Elena Buchatskaya, Trevor Cai, Eliza Rutherford, Diego de Las Casas, Lisa Anne Hendricks, Johannes Welbl, Aidan Clark, et al. Training compute-optimal large language models. *arXiv preprint arXiv:2203.15556*, 2022.
- [46] Prateek Yadav, Derek Tam, Leshem Choshen, Colin A. Raffel, and Mohit Bansal. Ties-merging: Resolving interference when merging models. In *NeurIPS*, 2023.
- [47] Yi Zhou, Parikshit Ram, Theodoros Salonidis, Nathalie Baracaldo, Horst Samulowitz, and Heiko Ludwig. Single-shot general hyper-parameter optimization for federated learning. In *The Eleventh International Conference on Learning Representations*, 2023.
- [48] Mikhail Khodak, Renbo Tu, Tian Li, Liam Li, Maria-Florina F Balcan, Virginia Smith, and Ameet Talwalkar. Federated hyperparameter tuning: Challenges, baselines, and connections to weight-sharing. *Advances in Neural Information Processing Systems*, 34, 2021.
- [49] Tian Li, Anit Kumar Sahu, Manzil Zaheer, Maziar Sanjabi, Ameet Talwalkar, and Virginia Smith. Federated optimization in heterogeneous networks. In *Proceedings of Machine Learning and Systems 2020, MLSys 2020*, 2020.
- [50] Qinbin Li, Bingsheng He, and Dawn Song. Model-contrastive federated learning. In *Proceedings of the IEEE/CVF Conference on Computer Vision and Pattern Recognition*, 2021.
- [51] Durmus Alp Emre Acar, Yue Zhao, Ramon Matas, Matthew Mattina, Paul Whatmough, and Venkatesh Saligrama. Federated learning based on dynamic regularization. In *International Conference on Learning Representations*, 2021.
- [52] Sai Praneeth Karimireddy, Satyen Kale, Mehryar Mohri, Sashank Reddi, Sebastian Stich, and Ananda Theertha Suresh. SCAFFOLD: Stochastic controlled averaging for federated learning. In *Proceedings of the 37th International Conference on Machine Learning*. PMLR, 2020.
- [53] Guan Wang, Charlie Xiaoqian Dang, and Ziyi Zhou. Measure contribution of participants in federated learning. In *IEEE International Conference on Big Data*. IEEE, 2019.

- [54] Tianhao Wang, Johannes Rausch, Ce Zhang, Ruoxi Jia, and Dawn Song. A principled approach to data valuation for federated learning. *Federated Learning: Privacy and Incentive*, 2020.
- [55] Yae Jee Cho, Jianyu Wang, and Gauri Joshi. Client selection in federated learning: Convergence analysis and power-of-choice selection strategies. *arXiv preprint arXiv:2010.01243*, 2020.
- [56] Jiyue Huang, Chi Hong, Lydia Y Chen, and Stefanie Roos. Is shapley value fair? improving client selection for mavericks in federated learning. *arXiv preprint arXiv:2106.10734*, 2021.
- [57] John Nguyen, Jianyu Wang, Kshitiz Malik, Maziar Sanjabi, and Michael Rabbat. Where to begin? on the impact of pre-training and initialization in federated learning. In *International Conference on Learning Representations*, 2023.
- [58] Hong-You Chen, Cheng-Hao Tu, Ziwei Li, Han Wei Shen, and Wei-Lun Chao. On the importance and applicability of pre-training for federated learning. In *International Conference on Learning Representations*, 2023.
- [59] Royson Lee, Minyoung Kim, Da Li, Xinchu Qiu, Timothy M. Hospedales, Ferenc Huszar, and Nicholas D. Lane. Fedl2p: Federated learning to personalize. In *Conference on Neural Information Processing Systems*, 2023.
- [60] Guangyu Sun, Matias Mendieta, Taojiannan Yang, and Chen Chen. Conquering the communication constraints to enable large pre-trained models in federated learning. *arXiv*, 2022.
- [61] Zhuo Zhang, Yuanhang Yang, Yong Dai, Qifan Wang, Yue Yu, Lizhen Qu, and Zenglin Xu. Fedpetuning: When federated learning meets the parameter-efficient tuning methods of pre-trained language models. In *Annual Meeting of the Association of Computational Linguistics 2023*, pages 9963–9977. Association for Computational Linguistics (ACL), 2023.
- [62] Jaehong Yoon, Geon Park, Wonyong Jeong, and Sung Ju Hwang. Bitwidth heterogeneous federated learning with progressive weight dequantization. In *International Conference on Machine Learning*, pages 25552–25565. PMLR, 2022.
- [63] Dezhong Yao, Wanning Pan, Michael J O’Neill, Yutong Dai, Yao Wan, Hai Jin, and Lichao Sun. Fedhm: Efficient federated learning for heterogeneous models via low-rank factorization. *arXiv preprint arXiv:2111.14655*, 2021.
- [64] Sebastian Caldas, Jakub Konečný, H Brendan McMahan, and Ameet Talwalkar. Expanding the reach of federated learning by reducing client resource requirements. *arXiv preprint arXiv:1812.07210*, 2018.
- [65] Yuang Jiang, Shiqiang Wang, Victor Valls, Bong Jun Ko, Wei-Han Lee, Kin K Leung, and Leandros Tassiulas. Model pruning enables efficient federated learning on edge devices. *IEEE Transactions on Neural Networks and Learning Systems*, 2022.
- [66] Royson Lee, Javier Fernandez-Marques, Shell Xu Hu, Da Li, Stefanos Laskaridis, Łukasz Dudziak, Timothy Hospedales, Ferenc Huszár, and Nicholas D Lane. Recurrent early exits for federated learning with heterogeneous clients. In *The 41st International Conference on Machine Learning*, 2024.
- [67] Minjae Kim, Sangyoon Yu, Suhyun Kim, and Soo-Mook Moon. DepthFL : Depthwise federated learning for heterogeneous clients. In *The Eleventh International Conference on Learning Representations*, 2023.
- [68] Fatih Ilhan, Gong Su, and Ling Liu. Scalefl: Resource-adaptive federated learning with heterogeneous clients. In *Proceedings of the IEEE/CVF Conference on Computer Vision and Pattern Recognition*, pages 24532–24541, 2023.
- [69] Kallista A. Bonawitz, Hubert Eichner, Wolfgang Grieskamp, Dzmitry Huba, Alex Ingerman, Vladimir Ivanov, Chloé Kiddon, Jakub Konečný, Stefano Mazzocchi, Brendan McMahan, Timon Van Overveldt, David Petrou, Daniel Ramage, and Jason Roselander. Towards federated learning at scale: System design. In *Proceedings of Machine Learning and Systems 2019*, *MLSys*, 2019.

- [70] Dzmityr Huba, John Nguyen, Kshitiz Malik, Ruiyu Zhu, Mike Rabbat, Ashkan Yousefpour, Carole-Jean Wu, Hongyuan Zhan, Pavel Ustinov, Harish Srinivas, Kaikai Wang, Anthony Shoumikhin, Jesik Min, and Mani Malek. PAPAAYA: practical, private, and scalable federated learning. In *Proceedings of the Fifth Conference on Machine Learning and Systems, MLSys 2022*, 2022.
- [71] Ewen Wang, Boyi Chen, Mosharaf Chowdhury, Ajay Kannan, and Franco Liang. FLINT: A platform for federated learning integration. In *Proceedings of the Sixth Conference on Machine Learning and Systems, MLSys 2023*. mlsys.org, 2023.
- [72] Yanli Zhao, Andrew Gu, Rohan Varma, Liang Luo, Chien-Chin Huang, Min Xu, Less Wright, Hamid Shojanazeri, Myle Ott, Sam Shleifer, Alban Desmaison, Can Balioglu, Pritam Damania, Bernard Nguyen, Geeta Chauhan, Yuchen Hao, Ajit Mathews, and Shen Li. Pytorch FSDP: experiences on scaling fully sharded data parallel. *Proc. VLDB Endow.*, 16(12):3848–3860, 2023. doi: 10.14778/3611540.3611569.
- [73] Shen Li, Yanli Zhao, Rohan Varma, Omkar Salpekar, Pieter Noordhuis, Teng Li, Adam Paszke, Jeff Smith, Brian Vaughan, Pritam Damania, and Soumith Chintala. Pytorch distributed: Experiences on accelerating data parallel training. *Proc. VLDB Endow.*, 13(12):3005–3018, aug 2020. ISSN 2150-8097. doi: 10.14778/3415478.3415530.
- [74] Zachary Charles, Nicole Mitchell, Krishna Pillutla, Michael Reneer, and Zachary Garrett. Towards federated foundation models: Scalable dataset pipelines for group-structured learning. In *Conference on Neural Information Processing Systems*, 2023.
- [75] Guanhua Wang, Heyang Qin, Sam Ade Jacobs, Connor Holmes, Samyam Rajbhandari, Olatunji Ruwase, Feng Yan, Lei Yang, and Yuxiong He. Zero++: Extremely efficient collective communication for giant model training. *arXiv preprint arXiv:2306.10209*, 2023.
- [76] Jie Ren, Samyam Rajbhandari, Reza Yazdani Aminabadi, Olatunji Ruwase, Shuangyan Yang, Minjia Zhang, Dong Li, and Yuxiong He. Zero-offload: Democratizing billion-scale model training. In *2021 USENIX Annual Technical Conference, USENIX ATC 2021*, pages 551–564. USENIX Association, 2021.
- [77] Samyam Rajbhandari, Jeff Rasley, Olatunji Ruwase, and Yuxiong He. Zero: memory optimizations toward training trillion parameter models. In *Proceedings of the International Conference for High Performance Computing, Networking, Storage and Analysis, SC 2020, Virtual Event Atlanta, Georgia, USA, November 9-19, 2020*, page 20. IEEE/ACM, 2020. doi: 10.1109/SC41405.2020.00024.
- [78] Alexander Borzunov, Dmitry Baranchuk, Tim Dettmers, Maksim Riabinin, Younes Belkada, Artem Chumachenko, Pavel Samygin, and Colin Raffel. Petals: Collaborative inference and fine-tuning of large models. In *Proceedings of the 61st Annual Meeting of the Association for Computational Linguistics: System Demonstrations, ACL 2023, Toronto, Canada, July 10-12, 2023*, pages 558–568. Association for Computational Linguistics, 2023. doi: 10.18653/V1/2023.ACL-DEMO.54.
- [79] Alexander Borzunov, Max Ryabinin, Artem Chumachenko, Dmitry Baranchuk, Tim Dettmers, Younes Belkada, Pavel Samygin, and Colin A. Raffel. Distributed inference and fine-tuning of large language models over the internet. In *Conference on Neural Information Processing Systems*, 2023.
- [80] Weirui Kuang, Bingchen Qian, Zitao Li, Daoyuan Chen, Dawei Gao, Xuchen Pan, Yuexiang Xie, Yaliang Li, Bolin Ding, and Jingren Zhou. Federatedscope-llm: A comprehensive package for fine-tuning large language models in federated learning. In *KDD*, pages 5260–5271. ACM, 2024.
- [81] Rui Ye, Wenhao Wang, Jingyi Chai, Dihan Li, Zexi Li, Yinda Xu, Yaxin Du, Yanfeng Wang, and Siheng Chen. Openfedllm: Training large language models on decentralized private data via federated learning. In *Proceedings of the 30th ACM SIGKDD Conference on Knowledge Discovery and Data Mining*, pages 6137–6147, 2024.

- [82] Sid Black, Stella Biderman, Eric Hallahan, Quentin Anthony, Leo Gao, Laurence Golding, Horace He, Connor Leahy, Kyle McDonell, Jason Phang, Michael Pieler, USVSN Sai Prashanth, Shivanshu Purohit, Laria Reynolds, Jonathan Tow, Ben Wang, and Samuel Weinbach. Gpt-neox-20b: An open-source autoregressive language model. *CoRR*, abs/2204.06745, 2022. doi: 10.48550/ARXIV.2204.06745.
- [83] Zhouyuan Huo, Qian Yang, Bin Gu, Lawrence Carin, and Heng Huang. Faster on-device training using new federated momentum algorithm. *CoRR*, abs/2002.02090, 2020.
- [84] Diego Granzio, Stefan Zohren, and Stephen Roberts. Learning rates as a function of batch size: A random matrix theory approach to neural network training. *J. Mach. Learn. Res.*, 23: 173:1–173:65, 2022.
- [85] Diego Granzio, Stefan Zohren, and Stephen Roberts. Learning rates as a function of batch size: A random matrix theory approach to neural network training. *J. Mach. Learn. Res.*, 23: 173:1–173:65, 2022.
- [86] Peter Clark, Isaac Cowhey, Oren Etzioni, Tushar Khot, Ashish Sabharwal, Carissa Schoenick, and Oyvind Tafjord. Think you have solved question answering? try arc, the AI2 reasoning challenge. *CoRR*, abs/1803.05457, 2018.
- [87] Aarohi Srivastava, Abhinav Rastogi, Abhishek Rao, Abu Awal Md Shoeb, Abubakar Abid, Adam Fisch, Adam R. Brown, Adam Santoro, Aditya Gupta, Adrià Garriga-Alonso, Agnieszka Kluska, Aitor Lewkowycz, Akshat Agarwal, Alethea Power, Alex Ray, Alex Warstadt, Alexander W. Kocurek, Ali Safaya, Ali Tazarv, Alice Xiang, Alicia Parrish, Allen Nie, Aman Hussain, Amanda Askell, Amanda Dsouza, Ambrose Slone, Ameet Rahane, Anantharaman S. Iyer, Anders Andreassen, Andrea Madotto, Andrea Santilli, Andreas Stuhlmüller, Andrew M. Dai, Andrew La, Andrew K. Lampinen, Andy Zou, Angela Jiang, Angelica Chen, Anh Vuong, Animesh Gupta, Anna Gottardi, Antonio Norelli, Anu Venkatesh, Arash Gholamidavoodi, Arfa Tabassum, Arul Menezes, Arun Kirubakaran, Asher Mullokandov, Ashish Sabharwal, Austin Herrick, Avia Efrat, Aykut Erdem, Ayla Karakas, B. Ryan Roberts, Bao Sheng Loe, Barret Zoph, Bartłomiej Bojanowski, Batuhan Özyurt, Behnam Hedayatnia, Behnam Neyshabur, Benjamin Inden, Benno Stein, Berk Ekmekci, Bill Yuchen Lin, Blake Howald, Bryan Orinion, Cameron Diao, Cameron Dour, Catherine Stinson, Cedrick Argueta, Cèsar Ferri Ramírez, Chandan Singh, Charles Rathkopf, Chenlin Meng, Chitta Baral, Chiyu Wu, Chris Callison-Burch, Chris Waites, Christian Voigt, Christopher D. Manning, Christopher Potts, Cindy Ramirez, Clara E. Rivera, Clemencia Siro, Colin Raffel, Courtney Ashcraft, Cristina Garbacea, Damien Sileo, Dan Garrette, Dan Hendrycks, Dan Kilman, Dan Roth, Daniel Freeman, Daniel Khoshdel, Daniel Levy, Daniel Moseguí González, Danielle Perszyk, Danny Hernandez, Danqi Chen, Daphne Ippolito, Dar Gilboa, David Dohan, David Drakard, David Jurgens, Debajyoti Datta, Deep Ganguli, Denis Emelin, Denis Kleyko, Deniz Yuret, Derek Chen, Derek Tam, Dieuwke Hupkes, Diganta Misra, Dilyar Buzan, Dimitri Coelho Mollo, Diyi Yang, Dong-Ho Lee, Dylan Schrader, Ekaterina Shutova, Ekin Dogus Cubuk, Elad Segal, Eleanor Hagerman, Elizabeth Barnes, Elizabeth Donoway, Ellie Pavlick, Emanuele Rodolà, Emma Lam, Eric Chu, Eric Tang, Erkut Erdem, Ernie Chang, Ethan A. Chi, Ethan Dyer, Ethan J. Jerzak, Ethan Kim, Eunice Engfu Manyasi, Evgenii Zheltonozhskii, Fanyue Xia, Fatemeh Siar, Fernando Martínez-Plumed, Francesca Happé, François Chollet, Frieda Rong, Gaurav Mishra, Genta Indra Winata, Gerard de Melo, Germán Kruszewski, Giambattista Parascandolo, Giorgio Mariani, Gloria Wang, Gonzalo Jaimovitch-López, Gregor Betz, Guy Gur-Ari, Hana Galijasevic, Hannah Kim, Hannah Rashkin, Hannaneh Hajishirzi, Harsh Mehta, Hayden Bogar, Henry Shevlin, Hinrich Schütze, Hiromu Yakura, Hongming Zhang, Hugh Mee Wong, Ian Ng, Isaac Noble, Jaap Jumelet, Jack Geissinger, Jackson Kernion, Jacob Hilton, Jaehoon Lee, Jaime Fernández Fisac, James B. Simon, James Koppel, James Zheng, James Zou, Jan Kocon, Jana Thompson, Janelle Wingfield, Jared Kaplan, Jarema Radom, Jascha Sohl-Dickstein, Jason Phang, Jason Wei, Jason Yosinski, Jekaterina Novikova, Jelle Bosscher, Jennifer Marsh, Jeremy Kim, Jeroen Taal, Jesse H. Engel, Jesujoba Alabi, Jiacheng Xu, Jiaming Song, Jillian Tang, Joan Waweru, John Burden, John Miller, John U. Balis, Jonathan Batchelder, Jonathan Berant, Jörg Frohberg, Jos Rozen, José Hernández-Orallo, Joseph Boudeman, Joseph Guerr, Joseph Jones, Joshua B. Tenenbaum, Joshua S. Rule, Joyce Chua, Kamil Kanclerz, Karen Livescu, Karl Krauth, Karthik Gopalakrishnan, Katerina Ignatyeva, Katja Markert, Kaustubh D. Dhole, Kevin Gimpel, Kevin Omondi, Kory Mathewson, Kristen Chiafullo, Ksenia Shkaruta, Kumar Shridhar, Kyle McDonell, Kyle

Richardson, Laria Reynolds, Leo Gao, Li Zhang, Liam Dugan, Lianhui Qin, Lidia Contreras Ochando, Louis-Philippe Morency, Luca Moschella, Lucas Lam, Lucy Noble, Ludwig Schmidt, Luheng He, Luis Oliveros Colón, Luke Metz, Lütfi Kerem Senel, Maarten Bosma, Maarten Sap, Maartje ter Hoeve, Maheen Farooqi, Manaal Faruqui, Mantas Mazeika, Marco Baturan, Marco Marelli, Marco Maru, María José Ramírez-Quintana, Marie Tolkiehn, Mario Giulianelli, Martha Lewis, Martin Potthast, Matthew L. Leavitt, Matthias Hagen, Mátyás Schubert, Medina Baitemirova, Melody Arnaud, Melvin McElrath, Michael A. Yee, Michael Cohen, Michael Gu, Michael I. Ivanitskiy, Michael Starritt, Michael Strube, Michal Swedrowski, Michele Bevilacqua, Michihiro Yasunaga, Mihir Kale, Mike Cain, Mimee Xu, Mirac Suzgun, Mitch Walker, Mo Tiwari, Mohit Bansal, Moin Amnaseri, Mor Geva, Mozdeh Gheini, Mukund Varma T., Nanyun Peng, Nathan A. Chi, Nayeon Lee, Neta Gur-Ari Krakover, Nicholas Cameron, Nicholas Roberts, Nick Doiron, Nicole Martinez, Nikita Nangia, Niklas Deckers, Niklas Muennighoff, Nitish Shirish Keskar, Niveditha Iyer, Noah Constant, Noah Fiedel, Nuan Wen, Oliver Zhang, Omar Agha, Omar Elbaghdadi, Omer Levy, Owain Evans, Pablo Antonio Moreno Casares, Parth Doshi, Pascale Fung, Paul Pu Liang, Paul Vicol, Pegah Alipoormolabashi, Peiyuan Liao, Percy Liang, Peter Chang, Peter Eckersley, Phu Mon Htut, Pinyu Hwang, Piotr Milkowski, Piyush Patil, Pouya Pezeshkpour, Priti Oli, Qiaozhu Mei, Qing Lyu, Qinlang Chen, Rabin Banjade, Rachel Etta Rudolph, Raefer Gabriel, Rahel Habacker, Ramon Risco, Raphaël Millière, Rhythm Garg, Richard Barnes, Rif A. Saurous, Riku Arakawa, Robbe Raymaekers, Robert Frank, Rohan Sikand, Roman Novak, Roman Sitelew, Ronan LeBras, Rosanne Liu, Rowan Jacobs, Rui Zhang, Ruslan Salakhutdinov, Ryan Chi, Ryan Lee, Ryan Stovall, Ryan Teehan, Rylan Yang, Sahib Singh, Saif M. Mohammad, Sajant Anand, Sam Dillavou, Sam Shleifer, Sam Wiseman, Samuel Gruetter, Samuel R. Bowman, Samuel S. Schoenholz, Sanghyun Han, Sanjeev Kwatra, Sarah A. Rous, Sarik Ghazarian, Sayan Ghosh, Sean Casey, Sebastian Bischoff, Sebastian Gehrmann, Sebastian Schuster, Sepideh Sadeghi, Shadi Hamdan, Sharon Zhou, Shashank Srivastava, Sherry Shi, Shikhar Singh, Shima Asaadi, Shixiang Shane Gu, Shubh Pachhigar, Shubham Toshniwal, Shyam Upadhyay, Shyamolima (Shammie) Debnath, Siamak Shakeri, Simon Thormeyer, Simone Melzi, Siva Reddy, Sneha Priscilla Makini, Soo-Hwan Lee, Spencer Torene, Sriharsha Hatwar, Stanislas Dehaene, Stefan Divic, Stefano Ermon, Stella Biderman, Stephanie Lin, Stephen Prasad, Steven T. Piantadosi, Stuart M. Shieber, Summer Mishserghi, Svetlana Kiritchenko, Swaroop Mishra, Tal Linzen, Tal Schuster, Tao Li, Tao Yu, Tariq Ali, Tatsu Hashimoto, Te-Lin Wu, Théo Desbordes, Theodore Rothschild, Thomas Phan, Tianle Wang, Tiberius Nkinyili, Timo Schick, Timofei Kornev, Titus Tunduny, Tobias Gerstenberg, Trenton Chang, Trishala Neeraj, Tushar Khot, Tyler Shultz, Uri Shaham, Vedant Misra, Vera Demberg, Victoria Nyamai, Vikas Raunak, Vinay V. Ramasesh, Vinay Uday Prabhu, Vishakh Padmakumar, Vivek Srikumar, William Fedus, William Saunders, William Zhang, Wout Vossen, Xiang Ren, Xiaoyu Tong, Xinran Zhao, Xinyi Wu, Xudong Shen, Yadollah Yaghoobzadeh, Yair Lakretz, Yangqiu Song, Yasaman Bahri, Yejin Choi, Yichi Yang, Yiding Hao, Yifu Chen, Yonatan Belinkov, Yu Hou, Yufang Hou, Yuntao Bai, Zachary Seid, Zhuoye Zhao, Zijian Wang, Zijie J. Wang, Zirui Wang, and Ziyi Wu. Beyond the imitation game: Quantifying and extrapolating the capabilities of language models. *Trans. Mach. Learn. Res.*, 2023, 2023.

- [88] Rowan Zellers, Ari Holtzman, Yonatan Bisk, Ali Farhadi, and Yejin Choi. Hellaswag: Can a machine really finish your sentence? In Anna Korhonen, David R. Traum, and Lluís Màrquez, editors, *Proceedings of the 57th Conference of the Association for Computational Linguistics, ACL 2019, Florence, Italy, July 28- August 2, 2019, Volume 1: Long Papers*, pages 4791–4800. Association for Computational Linguistics, 2019. doi: 10.18653/V1/P19-1472.
- [89] Yonatan Bisk, Rowan Zellers, Ronan Le Bras, Jianfeng Gao, and Yejin Choi. PIQA: reasoning about physical commonsense in natural language. In *The Thirty-Fourth AAAI Conference on Artificial Intelligence, AAAI 2020, The Thirty-Second Innovative Applications of Artificial Intelligence Conference, IAAI 2020, The Tenth AAAI Symposium on Educational Advances in Artificial Intelligence, EAAI 2020, New York, NY, USA, February 7-12, 2020*, pages 7432–7439. AAAI Press, 2020. doi: 10.1609/AAAI.V34I05.6239.
- [90] Keisuke Sakaguchi, Ronan Le Bras, Chandra Bhagavatula, and Yejin Choi. Winogrande: An adversarial winograd schema challenge at scale. In *The Thirty-Fourth AAAI Conference on Artificial Intelligence, AAAI 2020, The Thirty-Second Innovative Applications of Artificial Intelligence Conference, IAAI 2020, The Tenth AAAI Symposium on Educational Advances in*

Artificial Intelligence, EAAI 2020, New York, NY, USA, February 7-12, 2020, pages 8732–8740. AAAI Press, 2020. doi: 10.1609/AAAI.V34I05.6399.

- [91] Christopher Clark, Kenton Lee, Ming-Wei Chang, Tom Kwiatkowski, Michael Collins, and Kristina Toutanova. Boolq: Exploring the surprising difficulty of natural yes/no questions. In Jill Burstein, Christy Doran, and Thamar Solorio, editors, *Proceedings of the 2019 Conference of the North American Chapter of the Association for Computational Linguistics: Human Language Technologies, NAACL-HLT 2019, Minneapolis, MN, USA, June 2-7, 2019, Volume 1 (Long and Short Papers)*, pages 2924–2936. Association for Computational Linguistics, 2019. doi: 10.18653/V1/N19-1300.
- [92] Todor Mihaylov, Peter Clark, Tushar Khot, and Ashish Sabharwal. Can a suit of armor conduct electricity? A new dataset for open book question answering. In Ellen Riloff, David Chiang, Julia Hockenmaier, and Jun'ichi Tsujii, editors, *Proceedings of the 2018 Conference on Empirical Methods in Natural Language Processing, Brussels, Belgium, October 31 - November 4, 2018*, pages 2381–2391. Association for Computational Linguistics, 2018. doi: 10.18653/V1/D18-1260.
- [93] Kin Ian Lo, Mehrnoosh Sadrzadeh, and Shane Mansfield. Generalised winograd schema and its contextuality. In Shane Mansfield, Benoît Valiron, and Vladimir Zamdzhiev, editors, *Proceedings of the Twentieth International Conference on Quantum Physics and Logic, QPL 2023, Paris, France, 17-21st July 2023*, volume 384 of *EPTCS*, pages 187–202, 2023. doi: 10.4204/EPTCS.384.11.
- [94] Denis Paperno, Germán Kruszewski, Angeliki Lazaridou, Quan Ngoc Pham, Raffaella Bernardi, Sandro Pezzelle, Marco Baroni, Gemma Boleda, and Raquel Fernández. The LAMBADA dataset: Word prediction requiring a broad discourse context. In *Proceedings of the 54th Annual Meeting of the Association for Computational Linguistics, ACL 2016, August 7-12, 2016, Berlin, Germany, Volume 1: Long Papers*. The Association for Computer Linguistics, 2016. doi: 10.18653/V1/P16-1144.
- [95] Melissa Roemmele, Cosmin Adrian Bejan, and Andrew S. Gordon. Choice of plausible alternatives: An evaluation of commonsense causal reasoning. In *Logical Formalizations of Commonsense Reasoning, Papers from the 2011 AAAI Spring Symposium, Technical Report SS-11-06, Stanford, California, USA, March 21-23, 2011*. AAAI, 2011.
- [96] Dan Hendrycks, Collin Burns, Steven Basart, Andy Zou, Mantas Mazeika, Dawn Song, and Jacob Steinhardt. Measuring massive multitask language understanding. In *ICLR. OpenReview.net*, 2021.

Appendix

In this appendix, we provide the details omitted in the main paper and more analyses and discussions.

- Appendix A: Hyperparameters we used for various experiments in our paper, including architectural details and both centralized and federated hyperparameters.
- Appendix B: Implementation details, which include i) full algorithms (pseudo-codes) of the proposed methods (subsection B.4); ii) implementation of wall time in the paper (subsection B.1).
- Appendix C: Additional discussions that are helpful for the readers to better understand the background, including federated optimization of LLM pre-training (subsection C.1).
- Appendix D: Additional evaluations of the systems, e.g., the downstream evaluations.

A Hyper-parameters

As shown in Table 4, we trained models ranging in size from 125 million parameters to 7 billion for the causal language modeling task. We used the tokenizer presented in [82] with a vocabulary size of 50 368. The local optimizer the clients use in our experiments is AdamW [41], while the server optimizer is FedMom [83]. For all of our non-DiLoCo experiments, we default to FedAvg with server learning rate 1.0 and server momentum 0.0. The hyperparameters we used are reported in Table 5. We chose to train decoder-only models, although our system could train any LLM architecture because they have become the de-facto standard in language modeling and text generation owed to their sample efficiency.

For the experiments using DiLoCo, we tuned the most important hyperparameter in the outer optimizer, i.e. the server learning rate $\eta_s \in \{0.1, 0.3, 0.5, 0.7\}$, while keeping the momentum coefficient fixed at $m = 0.7$. The results of this tuning are shown in Figure 8. In order to achieve both the target values of perplexity, the only value which didn't bring exploding loss was $\eta_s = 0.1$.

We also note that the billion-scale experiments assume intermittent client availability, reflecting real-world scenarios in which participants may occasionally allocate free computing resources to federated pre-training. To accommodate this, we employ a stateless local optimization procedure, and resetting optimizer states each round. This enables *Photon* to operate seamlessly in sparse-compute scenarios, unlike standard distributed data parallelism (DDP), which requires fully dedicated and synchronized GPU workers. Stateless local optimization also eliminates the communication costs of synchronizing optimizer states, making it easier to ensure that federated pre-training remains compute-bound.

Table 4: Architecture details and local training parameters for our 125M, 350M, 1.3B, 3B, and 7B models. We report the number of transformer blocks, hidden model dimension d , number of attention heads, the linear layer expansion ratio, and Adam's parameters (β_1 and β_2). We also report the vocabulary size of the tokenizer we used [82] and the sequence length l .

| Model Size | #Blocks | d | #Heads | Exp. Ratio | (β_1, β_2) | Vocab | l |
|-------------|---------|------|--------|------------|----------------------|--------|------|
| 75M | 3 | 896 | 16 | 4 | (0.9, 0.95) | 50 368 | 1024 |
| 125M | 12 | 768 | 12 | 4 | (0.9, 0.95) | 50 368 | 2048 |
| 350M | 24 | 1024 | 16 | 4 | (0.9, 0.95) | 50 368 | 2048 |
| 1.3B | 24 | 2048 | 16 | 4 | (0.9, 0.95) | 50 368 | 2048 |
| 3B | 32 | 2560 | 20 | 4 | (0.9, 0.95) | 50 368 | 2048 |
| 7B | 32 | 4096 | 32 | 4 | (0.9, 0.95) | 50 368 | 2048 |

Table 5: Hyperparameters used in our experiments. The federated learning rate η_s and momentum μ_s [83] are applied by the *Photon* Agg. S_C are the parameters of the learning rate scheduler synchronized across **sequential** steps. α is the factor to be applied to the maximum learning rate η_{max} to obtain the minimum learning rate for the cosine scheduler, i.e., $\eta_{min} = \alpha \times \eta_{max}$. T is the duration, in steps, of the cosine scheduler for fed/cent variants. We also report the batch size used in the local training by the *Photon* clients and the centralized batch size.

| Model Size | η_s | μ_s | α | η_{max} | T | T_{cent} | Batch Size | Batch Size Cent |
|-------------|--------------------------------|------------|-----------|----------------------|--------|------------|------------|-----------------|
| 125M | {0.0, 0.1, 0.3, 0.5, 0.7, 1.0} | {0.9, 0.0} | 10^{-1} | 6.0×10^{-4} | 40 960 | 5120 | 32 | 256 |
| 1.3B | 1.0 | 0.0 | 10^{-1} | 2×10^{-4} | 24 800 | 24 800 | 512 | 512 |
| 3B | 1.0 | 0.0 | 10^{-1} | 1.6×10^{-4} | 51 500 | 51 500 | 512 | 512 |
| 7B | 1.0 | 0.0 | 10^{-1} | 1.2×10^{-4} | 63 900 | 63 900 | 1024 | 1024 |

Table 6: Hyperparameters for our federated experiments. P represents the total number of clients per federations, K the number of clients sampled per round, D the dataset, τ the number of steps per round.

| Model Size | P | K | D | τ |
|-------------|------------------|------------------|------------------------|--------------|
| 125M | {1, 2, 4, 8, 16} | {1, 2, 4, 8, 16} | C4 [40], The Pile [42] | 64, 128, 512 |
| 1.3B | 8 | 8 | C4 [40] | 500 |
| 3B | 4 | 4 | C4 [40] | 500 |
| 7B | 4 | 4 | C4 [40] | 500 |

B Implementation details

B.1 Modeling Wall Time

We implement a comprehensive wall time model to analyze the temporal efficiency of our federated learning system across different communication architectures. The wall time calculations account for both computation and communication costs, considering factors such as local training time, model broadcast time, gradient collection time, and aggregation overhead.

Local Training Time The local training time (T_L) for each client is determined by the number of local training steps and the client’s computational throughput:

$$T_L = \frac{\tau}{\nu}, \quad (1)$$

where τ represents the number of local training steps and ν is the local throughput measured in batches per second. Notably, T_L doesn’t scale with the number of clients per round K as we assume the ideal case where they all execute the same local training recipe in parallel on equipollent hardware. In our experiments, τ represents a hyperparameter that we vary to observe its influence on the final performance. During deployment, τ is one of the most important hyperparameters to tune to achieve a pre-defined objective, i.e., target perplexity value at some target wall time. The value of ν depends on the computing resources available and the distributed strategy that *Photon* adopts at local clients. Throughout our evaluation of the 125M parameter model, we used an empirical value of $\nu = 2$ batches per second for both centralized and federated models. For the 1B model, we used an empirical ν value of 0.147 for federated models and 0.839 for centralized models. For the 3B model, we used $\nu = 0.144$ and 0.395 respectively, and for the 7B model, we used $\nu = 0.032$ and $\nu = 0.12$.

Communication Time The communication overhead varies based on the chosen architecture. We implement a bandwidth scaling factor for systems with more than θ channels (default: 100) to account for network congestion.

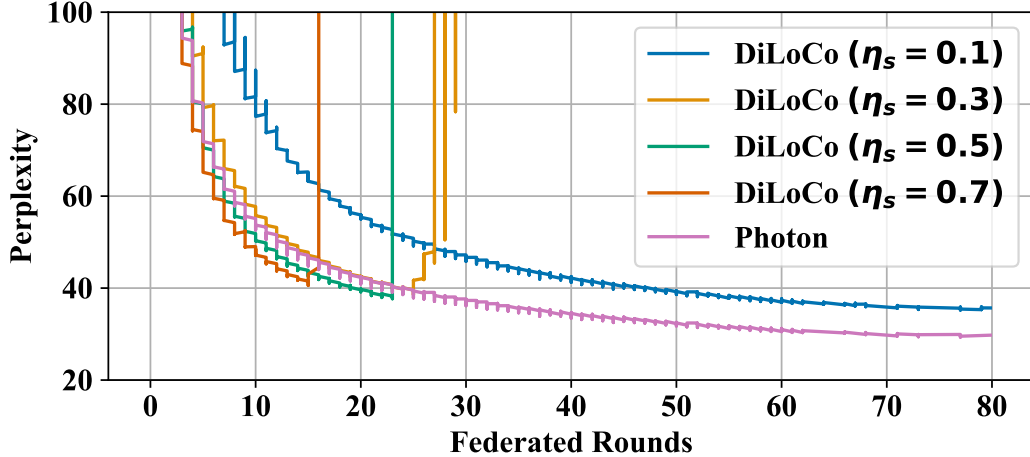


Figure 8: **Perplexity convergence comparison between *Photon* and *DiLoCo*.** We tuned *DiLoCo*’s recommended server optimizer (`OuterOpt`), SGD with Nesterov momentum, using learning rates $\eta_s \in \{0.1, 0.3, 0.5, 0.7\}$, while keeping the momentum coefficient fixed at 0.9. A 125M-parameter model was trained with a global batch size $B_g = 128$ and $N = 4$ clients per round. Higher η_s values accelerated training but hindered achieving the desired perplexity due to early divergent activations. Consequently, we set $\eta_s = 0.1$ in later experiments to reach lower perplexities.

For Parameter Server (PS) architecture, the total communication time (T_C^P) is:

$$T_C^{PS} = \begin{cases} \frac{KS}{B} & \text{if } K \leq \theta; \\ \frac{KS}{B} & \text{if } K > \theta, \end{cases} \quad (2)$$

where:

- K is the number of clients per round;
- S is the model size in megabytes;
- B is the server bandwidth in MBps.

For AllReduce (AR) architecture, the communication time (T_C^{AR}) is:

$$T_C^{AR} = \frac{(K-1)S}{B}, \quad (3)$$

For Ring AllReduce (RAR), we optimize the communication pattern, resulting in:

$$T_C^{RAR} = \frac{2S(K-1)}{KB}. \quad (4)$$

We admit that accounting for congestion and real-world measurements could further improve these models. However, we find them to provide sufficiently accurate results.

Total Wall Time The total wall time for one round (T_r) combines local computation and communication costs:

$$T_r^\alpha = T_L + T_C^\alpha, \quad (5)$$

where $\alpha \in \{PS, AR, RAR\}$ represents the chosen architecture.

The total wall time for the entire training process (T) is:

$$T^\alpha = RT_r^\alpha, \quad (6)$$

where R is the total number of federated learning rounds.

The aggregation time T_{agg} is calculated by:

$$T_{agg} = \frac{KS}{\zeta}, \quad (7)$$

where ζ is the server computational capacity. The default value of ζ is 5TFLOPS per second. For simplicity, the aggregation time at the server is currently considered negligible compared to communication costs, as shown in Equation 6. Still, the model allows for future extensions to include server-side computational overhead in cases where its computational capabilities are highly constrained. Our implementation accounts for exceptional cases as well, such as single-client scenarios without communication.

B.2 Overlapping communication and cleaning up

When partial participation is involved in the federated setting, clients may sporadically become available or drop out of the federation at any time. When they disconnect after they finish executing their local work for a specific federated round, the *Photon* LLM Client can offload the communication process and simultaneously clean up the memory allocated by the training pipeline to allow for the prompt return to idle state. This routine quickly makes computing resources available for another workload, which is particularly important when using shared computing facilities.

B.3 Advanced sharing for reducing memory footprint

Every *Photon* LLM Client comprises a multiprocessing stack managed by a leader process that coordinates subordinate processes handling the hardware accelerators. Such a leader process is also in charge of the communication endpoint, so it receives and sends model parameters as the algorithm requires. To minimize the RAM footprint up to $8\times$, the model parameters exchanged are stored in shared memory, accessible by all subordinate processes.

B.4 Full Algorithms

Algorithm 2 Distributed Data Parallel (DDP) Training Algorithm

Require: N : Number of devices (workers), f_θ : Model with parameters θ , T : Number of epochs

Require: \mathcal{D} : Dataset partitioned across devices \mathcal{D}_i where $i \in \{1, 2, \dots, N\}$

Require: RingAllReduce: All-reduce operation to aggregate across devices on a ring

Require: Opt: Optimizer for updating θ with gradients

- 1: **Initialize:** Randomly initialize model parameters θ_0 on each device
 - 2: **for** $t = 1$ to T **do**
 - 3: **Step 1: Parallel Local Training**
 - 4: **for** each device $i \in \{1, 2, \dots, N\}$ **in parallel do**
 - 5: Compute local mini-batch loss $\mathcal{L}_i(\theta_{t-1}, \mathcal{D}_i)$
 - 6: Compute local gradients $\nabla_{\theta_{t-1}} \mathcal{L}_i(\theta_{t-1})$
 - 7: **Step 2: Distributed RingAllReduce Gradient Aggregation**
 - 8: $\nabla_{\theta_{t-1}} \mathcal{L} = \frac{1}{N} \sum_{i=1}^N \nabla_{\theta_{t-1}} \mathcal{L}_i$
 - 9: Each device now possesses the global gradient $\nabla_{\theta_{t-1}} \mathcal{L}$
 - 10: **Step 3: Parallel Model Update**
 - 11: **for** each device $i \in \{1, 2, \dots, N\}$ **in parallel do**
 - 12: $\theta_t = \text{Opt}(\theta_{t-1}, \nabla_{\theta_{t-1}} \mathcal{L})$
 - 13: **Output:** Trained model parameters θ_T
-

Algorithm 3 Cross-silo Federated Learning (FL) Algorithm

Require: N : Number of clients, f_θ : Model with parameters θ , T : Number of federated rounds, K : Number of local steps

Require: $\{\mathcal{D}_i\}$: Federated dataset, i.e., a set of private \mathcal{D}_i , $i \in \{1, \dots, N\}$

Require: ClientOpt: local client optimizer, ServerOpt: server optimizer

- 1: **Initialize:** Randomly initialize global model parameters θ_0 on the server
 - 2: **for** $t = 1$ to T **do**
 - 3: **Step 1: Broadcast model parameters**
 - 4: Server sends θ_t to all N clients
 - 5: **Step 2: Parallel Local Training**
 - 6: **for** each client $i \in \{1, 2, \dots, N\}$ **in parallel do**
 - 7: $\omega_{i,0} \leftarrow \theta_{t-1}$
 - 8: **for** each local iteration $k \in \{1, 2, \dots, K\}$ **do**
 - 9: Compute local mini-batch loss $\mathcal{L}_i(\omega_{i,k-1}, \mathcal{D}_i)$
 - 10: Compute local gradients $\nabla_{\omega_{i,k-1}} \mathcal{L}_i(\omega_{i,k-1})$
 - 11: $\omega_{i,k} \leftarrow \text{ClientOpt}(\omega_{i,k-1}, \nabla_{\omega_{i,k-1}} \mathcal{L}_i(\omega_{i,k-1}))$
 - 12: $\Delta\theta_{t-1,i} \leftarrow \omega_{i,K} - \theta_{t-1}$
 - 13: **Step 3: Global Model Update (on the server)**
 - 14: $\theta_t = \text{ServerOpt}(\theta_{t-1}, \{\Delta\theta_{t-1,i}\})$
 - 15: **Output:** Trained model parameters θ_T
-

C Extended Discussion

C.1 Federated Optimization of LLM Pre-training

Federated optimization differs significantly from standard data-parallel training due to infrequent synchronization, which affects the multitude of assumptions upon which centralized pre-training of LLMs is built. In a centralized context, previous works have shown the following: (a) the number of parameters $|\theta|$ and the number of tokens T seen by the model should be scaled roughly equally [45] for compute-optimal training; (b) the batch size \mathcal{B} should be chosen based on the available hardware resources, with larger batch sizes providing benefits until a critical batch size $\mathcal{B}_{\text{crit}}$, is reached [44]; (c) the learning rate should be scheduled using cosine decay with a period equal to the total number of optimization-steps/batches T/\mathcal{B} . All of these components need to be modified for effective federated optimization.

From a theoretical perspective, infrequent parameter averaging methods such as Local SGD [24] or FedAvg [15] are expected to provide an effect similar to scaling the batch size in a centralized setting [33] when scaling the number of clients per round, however, given the many moving parts of the centralized recipe obtaining such improvements requires successfully adapting it to a federated context. We need to distinguish between the batch size of a given client \mathcal{B}_c and the effective batch size of a given round $\mathcal{B}_{\text{eff}} = \sum_{c \in C_r} \mathcal{B}_c$, which depends on the batch size of all sampled clients. While smaller batch sizes are known to provide generalization benefits [35], for the sake of efficiency, using the largest batch size that can fit inside a given accelerator is preferable. Thus, we assume that each client uses a fixed \mathcal{B}_c determined by their hardware and that, for the sake of simplicity, all clients have access to the same hardware

$$\mathcal{B}_i = \mathcal{B}_j, \forall i, j \in C \times C.$$

In cases where clients have sufficiently powerful hardware, we assume that they use a batch size $\mathcal{B}_c = \mathcal{B}_{\text{crit}}$ to avoid wasting compute. With this simplifying assumption, the compute-time trade-off in federated optimization depends only on the number of clients sampled in a given round $|C_r|$ and the number of local iterations T_c performed on each client, both assumed constant. In the case of $T_c = 1$, this coincides, when assuming full participation, with the centralized setting, allowing the critical batch size $\mathcal{B}_{\text{crit}}$ to be determined using the gradient noise scale as done in the work of McCandlish et al. [44]. We perform numerous experiments to understand how the number of local steps T_c changes the Pareto-frontier of the compute-time trade-off.

Assuming that the findings of Hoffmann et al. [45] hold in a federated context, the compute-optimal number of total steps, $T = R \times T_c$, that should be performed depends on the number of tokens appropriate for the given model size, roughly $20 \times |\theta|$ according to the work of Hoffmann et al. [45], and on the effective batch size as follows:

$$R \times T_c = \frac{20 \times |\theta|}{\mathcal{B}_{\text{eff}}}, \tag{8}$$

with the large caveat that this compute-optimal point was chosen, assuming that training would be conducted using the centralized critical batch size. However, accounting for this in the learning rate schedule is not trivial for two reasons. First, the averaging-based aggregation procedure will limit the impact of any individual update. This is true both from a simple mathematical perspective, the norm of the average update being less than the average of the update norms, and because client updates in federated learning have been shown to produce near-orthogonal updates which tend to result in small pseudo-gradient norms [43]. Second, clients take several optimization steps using their hardware-determined batch size before aggregation, with smaller batch sizes being known to require smaller learning rates [44] in centralized settings. Since we expect the client hardware batch size to be generally smaller than $\mathcal{B}_{\text{crit}}$, they are likely to fall in the regime of small-batch training. Thus, in our work, we propose decaying the learning rate following a cosine scheduler appropriate for the hardware batch size \mathcal{B}_c , using Eq. (8) to obtain the period by replacing \mathcal{B}_{eff} with \mathcal{B}_c . Having fixed this period, we only have to tune one hyperparameter in the form of the maximum learning rate η_{max} with the minimum learning rate being computed as $\eta_{\text{min}} = \frac{\eta_{\text{max}}}{10}$. In contrast, we find that neither square root nor linear learning rate scaling [84, 85] sufficiently stabilize centralized training across varying batch sizes.

Table 7: In-context learning comparison between *Photon* models. Our biggest model wins 6 out of 7 comparisons in this group.

| Name | ARC-Challenge [86] | BigBench QA Wikidata [87] | HellaSwag [88] | PIQA [89] | Winogrande [90] | ARC-Easy [86] | BoolQ [91] |
|-------------------------|--------------------|---------------------------|----------------|--------------|-----------------|---------------|--------------|
| <i>Photon-7B</i> | 0.265 | 0.447 | 0.524 | 0.729 | 0.522 | 0.508 | 0.530 |
| <i>Photon-3B</i> | 0.247 | 0.360 | 0.455 | 0.705 | 0.512 | 0.461 | 0.591 |
| <i>Photon-1B</i> | 0.243 | 0.215 | 0.349 | 0.676 | 0.516 | 0.390 | 0.612 |

Table 8: In-context learning comparison between *Photon* models. Our biggest model wins 5 out of 6 comparisons in this group.

| Name | Openbook QA [92] | Winograd [93] | LAMBADA (OpenAI) [94] | Bigbench [87] Strategy QA | COPA [95] | MMLU [96] |
|-------------------------|------------------|---------------|-----------------------|---------------------------|--------------|--------------|
| <i>Photon-7B</i> | 0.358 | 0.681 | 0.457 | 0.466 | 0.710 | 0.263 |
| <i>Photon-3B</i> | 0.316 | 0.656 | 0.381 | 0.464 | 0.620 | 0.252 |
| <i>Photon-1B</i> | 0.274 | 0.604 | 0.298 | 0.470 | 0.630 | 0.248 |

The momenta stabilize the local optimization direction for a given local momentum-based optimizer, such as AdamW [41]. Since they are generally implemented using exponential decay, the impact of any individual gradient step is reduced. In the case of federated optimization, this poses a challenge as we aim to update the momentum vectors to reflect the information received during the aggregation step. Directly communicating and averaging the momenta of all clients would increase the communication costs by the number of momenta of the optimizer relative to transmitting only the parameters, e.g., it would be three times higher for AdamW. To avoid such increases in communication costs, we keep the momenta local and rely on only the parameter update to regularize training.

D Additional Evaluation

D.1 Downstream evaluation of *Photon*'s models

To evaluate the downstream task performance of our models, we test across a series of in-context learning benchmarks. Our results, shown in Tables 7 and 8, demonstrate that the downstream performance of models trained with *Photon* scales as expected with model size, with our largest model winning 10 out of 14 comparisons. This proves the downstream utility of *Photon* models even when using a pre-training dataset not optimized for downstream performance. We expect that as we increase the model size and incorporate a broader and more qualitative data mixture, the downstream performance of *Photon* models will keep improving.

D.2 Communication Efficiency and Scalability

We present additional results on the communication efficiency and scalability of *Photon* when using 64 local steps per round (Fig. 9) and 128 local steps per round (Fig. 10). While using 128 steps results in a slightly increased total computational load due to minor reductions in convergence speed, reducing communication frequency by half significantly lowers the communication burden, particularly with higher numbers of clients per round. This trend is especially pronounced in communication-inefficient PS implementations and also applies to the faster RAR and AR methods.

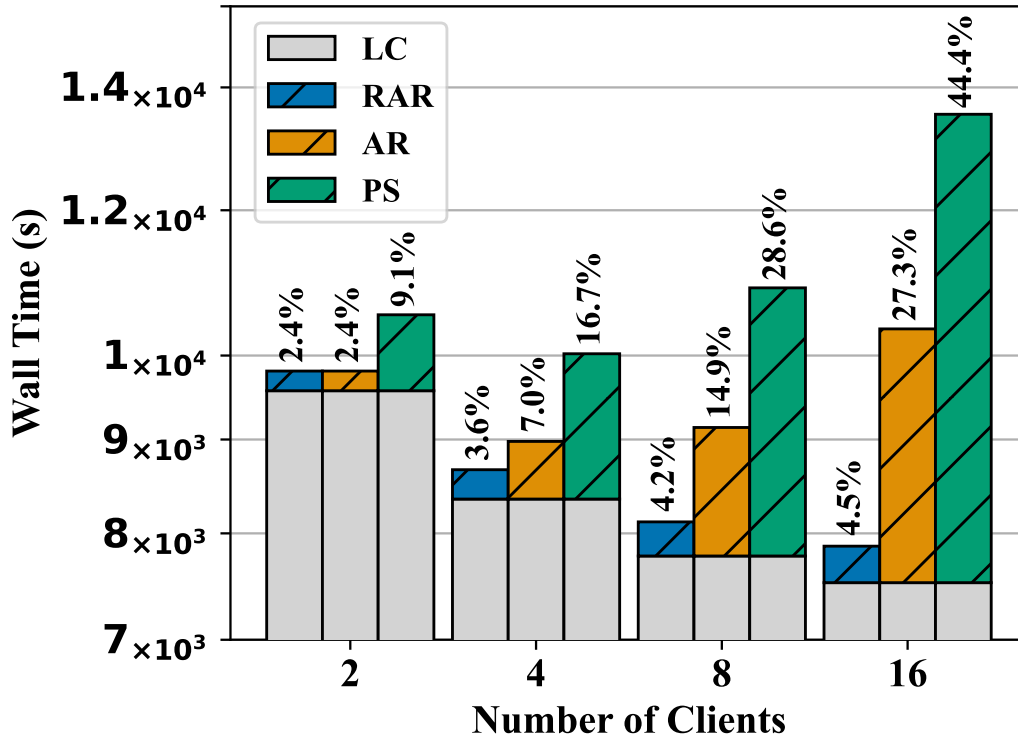


Figure 9: We report the split of the total wall time in two parts: the local compute time (LC) the clients endure to achieve the desired perplexity value and the communication time. The communication time is reported for three different aggregation implementations: *parameter server* (PS), which is necessary when privacy constraints are present; *AllReduce* (AR), more scalable than PS; *Ring-AllReduce* (RAR), the most scalable approach bounded by the slowest link across the ring topology. As we expected, communication represents a more important cost as the number of clients increases. Still, when implemented efficiently (RAR), the wall time benefits of scaling the computing resources are maintained. At the top of each bar, we report the percentage of time spent communicating for the respective experiments and implementation.

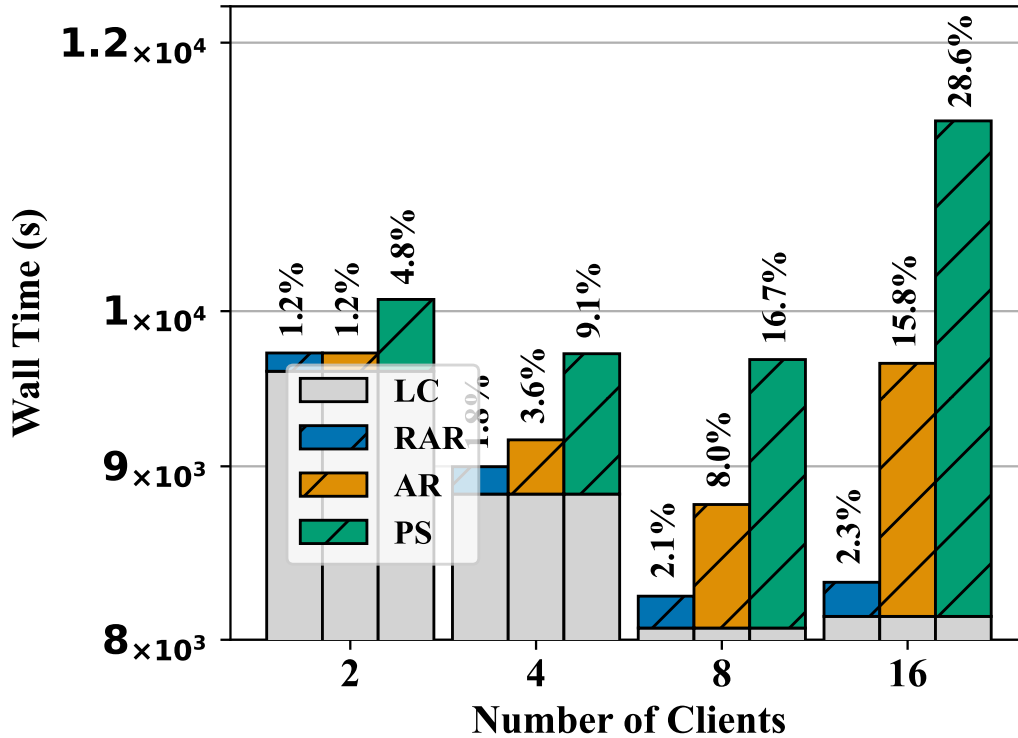


Figure 10: We report the split of the total wall time in two parts: the local compute time (LC) the clients endure to achieve the desired perplexity value and the communication time. The communication time is reported for three different aggregation implementations: *parameter server* (PS), which is necessary when privacy constraints are present; *AllReduce* (AR), more scalable than PS; *Ring-AllReduce* (RAR), the most scalable approach bounded by the slowest link across the ring topology. As we expected, communication represents a more important cost as the number of clients increases. Still, when implemented efficiently (RAR), the wall time benefits of scaling the computing resources are maintained. At the top of each bar, we report the percentage of time spent communicating for the respective experiments and implementation.